

UC Davis

UC Davis Electronic Theses and Dissertations

Title

Transcriptomic profile of the adult bovine ovary during pregnancy and different stages of the estrus cycle at the single cell resolution

Permalink

<https://escholarship.org/uc/item/7j4231w7>

Author

Weldon, Bethany

Publication Date

2023

Peer reviewed|Thesis/dissertation

Transcriptomic Profile of the Adult Bovine Ovary During Pregnancy and Different Stages
of the Estrus Cycle at the Single Cell Resolution

By

BETHANY WELDON
DISSERTATION

Submitted in partial satisfaction of the requirements for the degree of

DOCTOR OF PHILOSOPHY

in

Animal Biology

in the

OFFICE OF GRADUATE STUDIES

of the

UNIVERSITY OF CALIFORNIA

DAVIS

Approved:

Anna C. Denicol, Chair

Stuart Meyers

Fabio Lima

Committee in Charge

2023

To the best boys in the entire world, Bailey and Winston.

ACKNOWLEDGMENTS

I would like to express my heartfelt gratitude to the following individuals and organizations for their invaluable support and assistance throughout my PhD. I am deeply thankful to my family for their unwavering encouragement, understanding, and patience during this journey. Your support has been my anchor. My unwavering gratitude goes to my sister, Alexis, who I spoke on the phone with almost every day. She has always been a pillar of support for me. My father who is my inspiration, and guiding voice. My brother who has always been incredibly supportive. Lastly, I want to thank my mother Roseanne, she is my biggest cheerleader.

I owe a debt of gratitude to Anna Denicol, my mentor/advisor, for her expert guidance, insightful feedback, and continuous encouragement. Her wisdom has been instrumental in shaping my work and encouraging me through some of the most difficult years. I want to thank my committee members Dr. Stuart Meyers and Dr. Fabio Lima for your invaluable time and advice throughout my degree.

I am fortunate to have worked alongside a dedicated team of colleagues who provided valuable insights, shared ideas, and contributed tirelessly to the success of this project. Specifically, I would like to thank Delia Soto for her help with my initial understanding of sequencing and the beginning of my project. I would like to thank Marissa for her unconditional support throughout my project. I am fortunate to have an extremely supportive lab, and everyone in it helped more than I can express in achieving this. I want

to also thank Carly Guiltinan for her moral and technical support throughout my journey of learning single cell sequencing. I wouldn't have been able to learn any of this without Michelle Pepping, and her patience and her technical input. Lastly, I want to thank Juliana Candelaria, without her I don't think I would have been able to finish this degree. Not only with her input on my experiments but also her incredible support. I would go on to thank everyone that minorly impacted me because, in my opinion, you are all so important to me, but that would take a lot of space. I hope that everyone knows how much they influenced my success.

To my friends who provided moral support, offered a listening ear, and cheered me on during moments of doubt—thank you for being there.

I want to acknowledge the future readers and reviewers who will engage with this work. Your feedback and engagement are greatly appreciated.

This project would not have been possible without the collective support, encouragement, and contributions of these wonderful individuals and entities. Thank you all for being a part of this endeavor.

TABLE OF CONTENTS

List of figures.....	vii
List of Abreviations.....	ix
Dissertation abstract.....	x
CHAPTER 1. Literature Review	1
1.2 Ovarian architecture.....	2
1.3 Ovarian follicles.....	3
1.4 Ovarian development and establishment of the follicular reserve.....	4
1.5 Ovarian physiology.....	5
1.6 Importance of stromal cells for ovarian physiology.....	11
1.7 Recruitment of theca cells into the follicular unit.....	12
1.8 Sonic hedgehog signaling in the ovary.....	15
1.9 References.....	17
CHAPTER 2. Single cell rna sequencing of the bovine ovary.....	21
2.2 Introduction.....	21
2.2 Materials and methods.....	23
2.2.1 Optimization of ovarian tissue dissociation to maximize viability in single cell suspensions.....	23
2.2.2 Tissue dissociation for single cell sequencing.....	24
2.2.3 ScrRNAseq and data preprocessing.....	25
2.2.4 Data analysis.....	26
2.2.5 Cluster identification.....	27
2.2.6 Sub clustering analysis.....	28
2.2.7 Preparation of ovarian tissue for immunohistochemical analysis.....	28
2.2.8 Immunohistochemical quantification.....	29
2.2.9 Statistical analysis of collagen intensity.....	30
2.3 Results.....	30
2.3.1 major cell types identified in the ovarian cortex based on single cell transcriptome.....	30
2.4 Discussion.....	32

2.5	References	42
CHAPTER 3. Deciphering cellular interactions in the ovary and potential origins of theca cells using single-cell transcriptomics		
3.1	Introduction	44
3.2	Materials and methods	45
3.2.1	Animal preparation	45
3.2.2	Tissue processing for single cell-RNA sequencing	46
3.2.3	Tissue cryopreservation	46
3.2.4	Single-cell RNA sequencing (scRNAseq) and data pre-processing	47
3.2.5	Cluster identification	48
3.2.6	CellChat interactions.....	49
3.3	Results.....	49
3.3.1	Cell types of adult bovine ovaries across the estrous cycle.....	49
3.3.2	Changes observed in the cortex and medulla between the follicular and luteal phases of the estrus cycle	50
3.3.3	Cell cluster interactions	51
3.4	Discussion.....	51
CHAPTER 4. Conclusion to the dissertation.....		
4.1	References	63

LIST OF FIGURES

Figure 1: The cell types that are present in the pregnant adult bovine ovary. Cells from two pregnant heifers were isolated and sequenced using 10x genomics. After quality control, filtration, and integration 12,587 cells were analyzed. A uniform manifold approximation and projection (UMAP) plot featuring the different clusters in the ovary. 36

Figure 2: Ovarian Specific clusters; A-B. Showcasing CYP11A1, associated with Theca cells, amount (in the form of a dotplot) as well as the location (in the form of a feature plot) of expression within all the cell clusters. C-G. Showcasing granulosa cell markers FSHR, CYP19A1, AMH, INHA, NR5A2, and FST expression levels (in the form of a dotplot) and the location (in the form of a feature plot) within all the cell clusters. H-N. Showing the expression levels and locations of genes associated with the sonic hedgehog pathway (IHH, PTCH1, SMO, GLI1, HHIP, TCF21)..... 38

Figure 3: Subpopulations within the Stromal Population. A) A uniform manifold approximation and projection (umap) of the stromal subpopulations. There are three clusters, extracellular matrix building, cell migration, and vasculature forming. These labels are notating the putative functions of these subpopulations within the stroma. B) The top 5 markers determined by pairwise comparisons are shown, with the expression level notated by color and the size noting the percentage of cells expressing that transcript. 40

Figure 4: Collagen distribution within the stromal subclusters. Violin plots depicting the expression levels of collagens 1,3-6 and fibronectin. 40

Figure 5: A) Abundance of Collagen IV and V within different regions of the ovarian cortex. Least square means of collagen IV (A1) and collagen V (A2) in each region evaluated. Overall, both collagen types were more abundant in the epithelium, followed by the tunica albuginea and the perifollicular region surrounding antral follicles. Within each graph, different superscripts indicate significant differences in collagen abundance. B) Analysis of Collagen IV and V abundance following IHC. B)1-2. Representative image showing one area used for measurement of collagen abundance within the perifollicular region and the pixel measurement of NovaRed positive staining in the same region. B)3-4 Representative image showing one area used for measurement of collagen abundance within the epithelium (black arrow) and tunica albuginea (white arrowheads) regions and the pixel measurement of NovaRed positive staining in the same regions..... 41

Figure 6: Cell distribution in the Bovine Ovarian Cortex: A) 1 The sixteen cell cluster types within the bovine ovarian cortex shown in a uniform manifold approximation and projection. A) 2 The top 5 expressed genes in the bovine ovarian cortex determined by a Wilcoxon Rank Sum test and showcased as a clustered dotplot. The percentage of cells expressing the gene are noted by dot size and expression level noted by color. B) 1 The eight cell clusters in the bovine ovarian medulla shown in a uniform manifold approximation and projection. B) 2 The top 5 expressed genes in the bovine ovarian medulla determined by a Wilcoxon Rank Sum test and shown as a clustered dotplot. . 57

Figure 7: Cell Type Proportions in the Follicular vs Luteal Phase: A) The cortex cell types and proportions in both the follicular and luteal phase of the estrous cycle. B) The medulla cell types in both the follicular and luteal phase of the estrous cycle. 58

Figure 8: CellChat interactions. The cell-cell communication network for five of the cell clusters in the cortex utilizing a database of ligand-receptor interactions. A. The theca interstitial cells are communicating the strongest with the granulosa cells, the proliferating cells, the putative migratory stromal cells, theca cells as well as immune cells. B. The proliferating cells are communicating the strongest with the putative migratory stromal cells as well as immune cells. C. Theca cells are communicating with several other clusters, the strongest with; granulosa cells, immune cells (T-cells), putative migratory stromal cells, and proliferating cells. Additionally, they are communicating at a smaller amount with; endothelial cells (lymph, and blood vessels) and macrophages. D. Putative migratory stromal cells are strongly communicating with proliferating cells and granulosa cells. E. Finally, the granulosa cells are interacting the strongest with immune cells (macrophages), putative migratory stromal cells, and proliferating cells. They are also communicating to a lesser extent with theca cells and endothelial cells. 60

Figure 9: Sonic Hedgehog Signaling in the Bovine Ovarian Cortex. A. Expression localization of IHH. B. Expression localization of PTCH1. C. Expression localization of SMO. D. Expression localization of GLI1. E. Expression localization of HHIP. F. Expression localization of TCF21..... **Error! Bookmark not defined.**

LIST OF ABBREVIATIONS

3-HSD --3 β -Hydroxysteroid dehydrogenase	IAP – Inhibitor of apoptosis
17-HSD – 17 β - Hydroxysteroid dehydrogenase	LH – Luteinizing hormone
ADAMTS-1 – A disintegrin and metalloproteinase with thrombospondin motifs 1	mTOR – mammalian target of rapamycin
ART – Assisted Reproductive Technologies	P450AROM – Aromatase
AMH -- Anti-Mullerian Hormone	P450c17 -- Cytochrome p450 17A1
BMP-15 – Bone morphogenetic protein 15	P450SCC – Cholesterol side chain cleavage enzyme
CDC – Center for Disease Control	PGE2 – Prostaglandin E2
CAMP – Cyclic adenosine monophosphate	PKA –Protein Kinase A
COX-2 – Cyclooxygenase-2	PKC – Protein Kinase C
CL – Corpus Luteum	PI3K –Phosphoinositide 3-kinase
DHH – Desert Hedgehog Signaling molecule	USDA – United States Department of Agriculture
DMSO —Dimethyl Sulfoxide	PTEN – phosphatase and tensin binding homolog
ECM – Extracellular Matrix	SDF -1 —Stromal derived factor 1
Foxo3a – Forkhead box O3	SSH- Sonic Hedgehog signaling molecule
FSH – Follicle stimulating hormone	StaR – Steroidogenic acute regulatory protein
FBS —Fetal Bovine Serum	TSC1 —TSC complex subunit 1
GDF-9 – Growth differentiation factor 9	TSC2 —TSC complex subunit 2
HBSS – Hanks Balanced Salt Solution	VEGF – Vascular endothelial growth factor
IHH -- Indian Hedgehog signaling molecule	

DISSERTATION ABSTRACT

This study delves into the intricate cellular landscape of the ovary, aiming to unravel the complexities of its various cell populations and their dynamics during the estrus cycle leveraging single-cell RNA sequencing. This dissertation achieves two primary objectives: first, identifying stromal cell subclusters and localization of novel collagens within the bovine ovary, and second, identifying unique cell types in the ovarian cortex and medulla while tracking their changes across different estrus cycle stages and probing into the origins of theca cells within the ovarian stroma. Major findings include the discovery of putative distinct cell types, such as theca interstitial cells and migratory stromal cells, along with shifts in cell proportions from the follicular to luteal phases. Notably, the presence of the hedgehog signaling pathway within the cortex confirms previous reports in cattle and other species and suggests a potential role in the follicular recruitment of theca cells. Furthermore, the investigation extends to the medullary region, uncovering diverse cell populations encompassing endothelial cells, smooth muscle cells, immune cells, neuronal cells, and stromal cells. The luteal phase emerges as a period marked by intense proliferation of endothelial cells, vital for angiogenesis and the sustained function of the corpus luteum. While this research enhances our comprehension of the ovarian microcosm, it also underscores the necessity of further functional exploration. Future endeavors will focus on delving deeper into the functional implications of these findings in the realm of reproductive biology and the advancement of assisted reproductive technologies.

CHAPTER 1. LITERATURE REVIEW

1.1 Introduction

The use of assisted reproductive technologies (ART) in livestock has increased the efficiency of genetic gain over the last 50 years due to its ability to circumvent issues such as geographical distance to move animals, the time interval between generations, and the inability to use deceased animal genetic material. According to the Centers for Disease Control and Prevention (n.d.), ART is defined as a collection of processes where a human handles either the sperm or the oocyte. Scientific research in reproductive physiology has led to the development of ARTs and, thus, over time, widespread adoption of ART practices in both human medicine and agricultural production. Moreover, as the use of this technology has been growing, further research has been prompted to improve its practices and expand its potential. In the United States, more than 60% of dairy cattle are reproduced using artificial insemination as an assisted reproductive technology (Smith et al., 2021). In the human reproduction field, as of 2019, 2.1% of all infants born in the United States were conceived using assisted reproductive technology, according to the Centers for Disease Control and Prevention (n.d.). As ARTs become more widely used and more extensive in nature, the gaps in our understanding of ovarian biology are becoming evident. More specifically, improving our knowledge about the cell populations that encompass the ovary, their functions, and relationships during the reproductive cycle will be critical to maximizing the chances of success in the ever-expanding field of assisted reproduction. The following literature review will cover the ovary in its entirety, including the structures found within and their changes over the estrous cycle. The original research presented in this dissertation aimed to characterize the adult bovine

ovary at the single-cell level during the follicular and luteal phases of the estrus cycle and during the first trimester of pregnancy. By examining the ovarian single-cell transcriptome, we began to unravel an understanding of cell populations within the ovarian stroma, which has been poorly characterized to date. We attempted to demonstrate how these populations interact with each other to accomplish ovarian function ultimately.

1.2 Ovarian Architecture

The ovary is the gonad of a female and has two main functions: to produce hormones and house the developing germ cells, termed “oocytes.” These functions are driven by the dynamic behavior of the ovary, which allows for necessary hormone fluctuations and timed production of mature oocytes during each reproductive cycle. The mammalian ovary undergoes predictable and large restructuring events every three to four weeks, depending on the species, setting it apart from any other organ in the body. Anatomically, the ovary contains two distinct regions: the cortex and the medulla. These regions are structurally unique, therefore also giving them unique functions. The surface epithelium is a single layer of cuboidal cells on the surface of the ovary, covering the cortex. It is keratin-rich and suggested to be responsible for wound regeneration-like function after ovulation as well as dynamic expansion and regression in response to alterations in the ovarian structure throughout the cycle (Auersperg et al., 2001). Directly below the surface epithelium is a thin protective collagen-rich sheath called the tunica albuginea; this structure also needs to undergo remodeling to allow for each ovulation cycle (Reeves, 1971; Okamura et al., 1980) Beneath the tunica albuginea resides the ovarian cortex which contains the ovarian follicles, the functional unit of the ovary. The most interior aspect of the ovary is the medulla, which primarily contains the vasculature and very

dense connective tissue (Williams et al., 2012). These structures are well conserved across livestock species, with the exception of the mare and some other members of the Perissodactylaperissodactyla order, where the cortex is in the center of the ovary, surrounded by the medulla (Arthur 1969). In these animals, the ovary is characterized by a discrete area where ovulation occurs, named the ovulation fossa (Carnevale et al., 1988).

1.3 Ovarian Follicles

As mentioned above, the ovarian cortex harbors various sizes of ovarian follicles, corresponding to distinct stages of development. Each follicle is made of an oocyte directly surrounded by the somatic support cells. The structure of the follicle changes gradually during development in the process called folliculogenesis. The ovarian reserve is composed of quiescent primordial follicles that form during fetal development in most species. Primordial follicles consist of a small primary oocyte surrounded by one layer of flattened granulosa cells. Primordial follicle activation is characterized by morphological and functional changes where granulosa cells become cuboidal, gain mitotic potential, and increase their metabolic activity; this follicle is then called a primary follicle (McNatty et al. 1999, 2007, Montgomery et al. 2001, Barnett et al. 2006, Edson et al. 2009). The oocyte undergoes gradual diameter and volume expansion as granulosa cells proliferate and form multiple layers. Follicles with 2-3 layers or 4+ layers of granulosa cells are considered early and, or full secondary, respectively. At this stage, theca cells are recruited from the stromal cell environment and surround the oocyte-granulosa cell structure outside the basement membrane. Finally, the follicle develops a fluid-filled cavity called the antrum, at which stage it enters the antral phase of folliculogenesis, which is

dependent on gonadotropin signaling. Prior to this, the follicle is gonadotropin-responsive and relies on paracrine and autocrine signaling for growth and development (Zeleznik, 2004). While the endpoint of folliculogenesis is mostly described as ovulation, the more common fate of the follicle is atresia as only 0.01% of all follicles established in the ovary at birth will yield a developmentally and meiotically competent oocyte (Zeleznik, 2004). After ovulation, theca cells luteinize to become small luteal cells, and granulosa cells become large luteal cells, together contributing to the two main cell types of the corpus luteum REF?. After regression of the corpus luteum, the corpus albicans forms and is made of connective tissue (primary collagen) and remains in the ovary for several months as a scar.

1.4 Ovarian Development and Establishment of the Follicular Reserve

The establishment of the ovarian follicular reserve begins in the embryo and consists of 3 major processes: 1) specification of the primordial germ cells during gastrulation, 2) migration and proliferation, and 3) colonization of the urogenital ridges by the primordial germ cells (Vanderhyden 2006). In the bovine, the formation of the genital ridge develops by day 28-32 of gestation (Noden et al., 1985). The genital crests do not contain any PCGs at their formation, and migration of the PCGs from the yolk sac needs to occur. PCGs migrate from the yolk sac to the genital ridge via ameboid movements using pseudopodia between days 30-64 of gestation (Russe et al., 1991). The migration of PCGs is controlled by chemotactic signals produced by the genital ridge, called kit ligand, and integrins (Oktem et al 2008; Buehr et al., 1993; Anderson et al., 1999). The migration of PCGs includes their replication. When they reach the ridge, there are over ten thousand, and their maximum number is around two million. After the PCGs migrate and

settle in the genital ridges, there is an invasion of epithelial proliferations in the mesenchyme of the genital ridges. These invasions give rise to the gonadal cords and medullar cords. These sex chords break apart to form cell clusters surrounded by somatic tissue, further developing into the rete ovarii (Lin et al., 2002). These cell clusters divide synonymously but with incomplete division of the cytoplasm, creating a syncytium. After many rounds of division, the DNA in the oogonia is replicated, and meiotic division is entered and then arrested in the diplotene stage, creating primary oocytes. As the development of the fetus continues, the large number of oocytes is decreased dramatically through apoptosis, from two million cells, there ends up being to only around 130,000 at birth (Erickson et al., 1966). Following meiotic division, epithelial cells from the sex chords send out cytoplasmic processes between the interconnected oogonia, separating the cluster of oogonia into individual oocytes surrounded by a layer of pre-granulosa cells. At the same time, a basal lamina is deposited on the surface of the granulosa cells, completely isolating the newly formed primordial follicles from the ovarian stroma. In bovine species, the fully formed individual primordial follicles are present around day 90 of gestation (Yang et al., 2008). After completion of the formation of the follicles, they are embedded in a matrix of fibroblasts, collagen, and elastin within the cortex of the ovary and will remain there until activated for growth.

1.5 Ovarian Physiology

Reproductive cyclicity is dependent on the tight regulation of the production of oocytes. This regulation is driven by changes in hormones produced by the hypothalamus, pituitary, and ovary. Female reproductive cycles can be broadly characterized as estrous or menstrual cycles, depending on species. The recruitment of the primordial follicle to

the primary follicle is not completely understood, but it's thought that paracrine communication between the oocyte, granulosa cells, adjacent stromal/thecal cells, and surrounding follicles all contribute to follicle activation. There is a tentative model of activation based on studies in murine species where two major signaling pathways within the oocyte, phosphatidylinositol 3-OH-kinase (PI3K)-AKT-foxo3a signaling and the mammalian target of rapamycin (mTOR) signaling, play a pivotal role in triggering the development of quiescent primordial follicles (Sullivan et al., 2011). In the mouse, a loss of phosphatase and tensin homolog (PTEN) in oocytes causes activation of primordial follicles, suggesting that activity of PTEN negatively regulates PI3K signaling, thus inhibiting activation (Reddy et al., 2008). In mice null for Foxo3a, global activation of primordial follicles occurs (Castrillon et al., 2003). Within the mTOR signaling pathway, there is a complex of tuberous sclerosis proteins, TSC1 and TSC2, that inhibit mTOR signaling to prevent activation (Adhikari et al., 2009). Stromal-derived factor-1 (SDF-1) also appears to have a role in an autocrine/paracrine fashion to inhibit follicle activation (Holt et al., 2006). Once in the primary stage, several hallmark steps critical events occur, such as the expression of the FSH receptor and the growth and differentiation of the oocyte (Oktay et al., 1997; Candelaria et al., 2020). The oocyte increases in diameter and develops the extracellular matrix and zona pellucida during the primary stage (Bachvarova et al., 1989). In addition to oocyte growth and differentiation, connections develop between the oocyte and granulosa cells (Albertini et al., 2001; Eppig 1994). These connections, named gap junctions, are made of connexins and allow for direct communication between the granulosa cells and the oocyte. The absence of gap junctions results in failed follicular growth and infertility (Bruzzone et al., 1996; Simon et

al., 1997) Transitioning from primary to secondary follicle includes the addition of a second layer of granulosa cells. This transition is regulated by GDF-9 and BMP-15 for granulosa cell recruitment and arrangement (Chang et al., 2002). As multiple layers of cells accumulate, gap junctions continue to develop to create a communicative unit of cells. While granulosa cells are contributing to the follicle, theca cells are also being recruited (Erickson et al., 1985). In the primary to secondary transition, two layers of theca cells appear, the theca interna and theca externa. The theca interna continues to develop into theca interstitial cells, and the outer theca externa cells develop into smooth muscle (Erickson et al., 1985). Along with theca development is the formation of small blood vessels, allowing for blood flow to reach the growing follicle. This marks the end of the preantral phase of follicular growth, with a fully-grown oocyte with a zona pellucida, multiple layers of granulosa cells, a basal lamina, both theca externa and interna with accompanying capillary net. The antral follicle is characterized by a fluid-filled cavity referred to as the "antrum." The fluid is more specifically referred to as follicular fluid, which is a plasma exudate that contains secretory products from the oocyte and granulosa cells (Edwards et al., 1974). The follicular fluid creates a microenvironment in which regulatory molecules must pass through to reach the oocyte and granulosa cells. In the process of cyclicity, there is a period where one antral follicle is selected to become the dominant follicle, known as selection. The antral stage of follicular growth, specifically the dominant follicle, has massive cell proliferation, as well as the antrum increases dramatically in size. Once the dominant follicle is selected, the other follicles within that cohort slow their growth and eventually undergo atresia (Danial et al., 2004). The mechanism of selection is the rise of plasma FSH a few days before the fall of

progesterone after the luteal phase. The major causes for the increase of FSH are decreased estradiol as well as inhibin A production from the CL. The abundance of antral follicles within the ovary varies over the course of an animal's life, and most follicles within the ovary will undergo atresia (Danial et al., 2004). Follicle survival is regulated by a balance of apoptotic factors and FSH regulation. FSH supports follicle growth and is necessary for follicle survival via downstream signaling pathways. More specifically, FSH activates the PI3K signaling pathway within the granulosa cells and there is an increase in phosphorylation of protein kinase B, as well as inhibitor of apoptosis (IAP) proteins, leading to a decrease in the intrinsic cell death pathway (Hussein 2005). The FSH receptor is a part of a large family of seven transmembrane receptors that regulate heterotrimeric G proteins (Simoni et al., 1997). After binding of FSH, there is a conformational shift within the transmembrane portion of the receptor that activates a heterodimer G protein that, therefore, generates cAMP and the downstream activation of cAMP-dependent protein kinase (PKA) (Gonzalez-Robayna et al., 2000). As the amount of FSH increases, the production of the enzyme P450AROM/aromatase increases, therefore increasing the production of estradiol (Simpson 2004). Aromatase is first detected around ~1mm of follicular size, and the activity increases progressively, reaching very high levels right before ovulation (Ghersevich et al., 1994; Sawetawan et al., 1994; Zhang et al., 1996). Within the dominant antral follicle, theca interna cells are epithelioid cells responsible for producing steroids, with the accompanying characteristics of steroid-producing cells, including a cytoplasm filled with lipid droplets, smooth endoplasmic reticulum and a mitochondrion with tubular cristae (Erickson et al., 1985). These cells also possess receptors for luteinizing hormone (LH) and insulin. In response

to insulin and LH, they produce high levels of androgens, the most notable being androstenedione (Erickson et al., 1993). Androstenedione is an intermediate androgen before being converted into estradiol. As the production of aromatase increases, the granulosa cells become highly active in converting theca-derived androstenedione to estradiol by aromatization. At the time of antrum formation, theca interstitial cells begin to express a multitude of proteins that include LH receptors, insulin receptors, lipoprotein receptors, steroidogenic acute regulatory protein (StAR), cholesterol side chain cleavage enzyme (P450SCC), 3-hydroxysteroid dehydrogenase (3-HSD), and cytochrome P450c17, and it is these genes that are imperative for androstenedione production. The LH receptor is structurally very similar to the FSH receptor, it is a G-protein coupled seven transmembrane receptor with an intracellular domain for PKC phosphorylation (Ascoli et al., 2002). There is a mechanism that refers to this process of hormone production from the dominant follicle called the “two-cell two-gonadotropin concept.” As LH is delivered to the theca interstitial cells, it leads to the synthesis and secretion of androstenedione; this androgen then diffuses through the basement membrane and across the plasma membrane of the mural granulosa cells where P450AROM, induced by FSH, catalyzes its aromatization to estrone and then conversion to estradiol by 17-HSD.

As the antral follicle develops, the LH receptor expression is suppressed in the cumulus granulosa cells, and expression is increased in the mural granulosa cells. FSH plays a critical role in LH receptor expression in granulosa cells. LH receptors are suppressed until later in the follicular phase of the cycle to control ovulation. The oocyte itself controls LH receptor expression, and the oocyte inhibits FSH-induced LH receptors (Erickson et al., 2000; Henriks et al., 2005). The pathophysiology for this control is to inhibit the

response of the follicle to LH until the preovulatory phase, where it can then respond to the LH surge. This LH surge triggers ovulation by changing the gene expression profiles of mural granulosa cells (Russell et al., 2007). Specifically, LH triggers the production of the protease ADAMTS-1 in granulosa cells where it functions to cleave extracellular matrix proteins (Russell et al., 2003). The granulosa cells that directly surround the oocyte are referred to as cumulus granulosa cells, and these respond to LH differently. These granulosa cells have a much lower expression of the LH receptor, and instead of responding to LH directly, they receive input indirectly from diffusible factors from the mural granulosa cells. In addition to LH, prostaglandins have an important role in ovulation, specifically prostaglandin E₂(PGE₂) (Athanasίου et al., 2006; Ben-Ami et al., 2006). PGE₂ is generated by the cumulus cells in response to cyclooxygenase-2 (COX-2), and inhibition of COX-2 results in a delay in ovulation (Ben-Ami et al., 2006). After ovulation, there is a hole in the ovarian surface that is known as the stigma that allows the egg and cumulus complex to leave the follicle. The development of the stigma results from a combination of apoptosis, cell migration, and digestion of the extracellular matrix (Kim et al., 2008; Chappell et al., 1997; Lydon et al., 1995). As this remodeling occurs, the theca layer goes through alterations in the vascular supply in response to LH. Antral follicle growth is accompanied by vascular endothelial growth (VEGF). The VEGF and its downstream signaling pathways are required for follicle angiogenesis during growth and seem to be important for follicle rupture as well (Levin et al., 1998). VEGF also promotes vascular permeability, this allows for more efficient delivery of LH, FSH, and immune cells to the follicle. Macrophages, leukocytes, and a host of other immune cells are delivered to the theca layer by vasculature, and they release cytokines and proteases that promote

additional remodeling of the follicular wall. All of these changes lead to the degradation of the stromal matrix that is blocking the follicle from ovulating, creating the stigma.

After ovulation, the corpus luteum (CL) is formed. The CL is an endocrine gland that produces large amounts of progesterone and, to a lesser extent, estradiol during the first week of the luteal phase. After ovulation, granulosa cells grow in size and are then referred to as granulosa-lutein cells or large luteal cells; theca cells become theca-lutein or small luteal cells. Both of these cells have the hallmark ultrastructure of steroid-producing cells, abundant smooth endoplasmic reticulum, tubular cristae in the mitochondria, and large clusters of lipid droplets containing cholesterol esters (Crisp et al., 1970). Granulosa-lutein cells produce a large amount of progesterone and estradiol by increasing StAR, P450AROM, P450SCC, and 3-HSD (Carr et al., 1982). The theca-lutein cells express P450c17 and P450AROM to increase the production of androstenedione. If there is no embryo implantation, the corpus luteum is destroyed by luteolysis. After all cells are destroyed within the corpus luteum, all that remains is a bit of dense connective tissue called the corpus albicans.

1.6 Importance of stromal cells for ovarian physiology

In the previous section, the process of folliculogenesis and the intricate signaling pathways that are involved in the estrous cycle were detailed. However, the ovarian stromal tissue was not quite represented. What is known about the stromal population is limited in this description. The parenchyma of the ovary consists solely of the ovarian follicle, where the oocyte is housed until ovulation, and the rest is denoted as stroma (Young et al., 2014; Mescher, 2018). The stroma is, in essence, everything that is not an

ovarian follicle, encompassing immune cells, blood vessels, lymphatic vessels, ovarian surface epithelium, tunica albuginea, hilar cells, and uncharacterized cells. There are tentative descriptions of these uncharacterized cells as fibroblast-like, spindle-shaped cells, and interstitial cells (Reeves 1971). Fibroblasts typically are responsible for the deposition of extracellular matrix (ECM) proteins, such as collagen, for scaffolding. The bovine ovary has a significant amount of ECM and is considered to be fibrous in nature. The main ECM proteins seen in the ovary are collagens I, III, IV, VI, fibronectin, and laminin (Berkholtz et al., 2006; Irving-Rodgers et al., 2006). These proteins are integral for forming networks to create the matrix in that the ovarian cells exist within. The distribution of these “stromal subtypes” is likely to fluctuate with location in the ovary as well as the time point during the cycle. There is evidence that the life stage also has a significant impact on the stromal population, which is evident with increasing amounts of fibrin as age increases. While we are beginning to understand the various stromal cell populations, there are still some large gaps in this knowledge.

1.7 Recruitment of theca cells into the follicular unit

As covered briefly, theca cells are first observed in secondary stage preantral follicles with two or more layers of granulosa cells (Young et al., 2010). The follicle in the antral stage is surrounded by layers of theca cells that are intermixed with vasculature and immune cells (Hatzirodos et al., 2014). Within the theca cell layers, there is a separation between the theca interna and the theca externa, with the former mainly responsible for steroidogenesis, vascular and immune support and the latter mainly comprised of fibroblast-like cells serving as structural support (Yamamoto et al., 1997). After ovulation, the theca cells invade the granulosa cell layers as well as the vasculature and immune

cells, forming the CL (Richards et al., 2017). In addition to forming the CL, a large portion of theca cells will undergo atresia (Irving-Rodgers et al., 2001). The molecular mechanics and selection criteria for theca cells to become recruited to the follicle still need to be investigated in greater detail. There are several proposed mechanisms as to when and how these cells are recruited. The first theory is that these cells are present in the newborn ovary as putative theca cells or theca stem cells (TSC). Honda et al, (2007) were able to isolate and purify putative thecal stem cells that formed characteristic anchor-dependent round colonies that, after stimulation, showed signs of steroidogenesis. They were able to sort for these cells purely based on culture conditions, although they were not able to culture these cells indefinitely. This could be due to the inherent nature of these cells or because of suboptimal culture conditions. They then transplanted these thecal stem cells back into the host ovary, and they were able to recolonize the ovary, similar to Leydig stem cells in mice and rats. The isolated putative thecal stem cells were able to participate in both the theca externa and theca interna, demonstrating the ability of these cells to differentiate and function within the ovarian tissue (Honda et al., 2007). The second theory is they are differentiating from embryonic progenitor cells that are pre-selected to become theca cells. This theory is based on a study that found two specific theca cell progenitors, the progenitor cells are either *Gli*⁺ or *Wt1*⁺ and acquire lineage markers in response to paracrine signals (Liu et al., 2015). In a comparison of the transcriptomes of these two proposed progenitor populations, genes associated with steroidogenesis (*Star*, *Cyp17a1*, *Cyp11a1*, *Lhgr*) were found to be enriched in the mesonephros-derived *Gli*⁺ cells. Conversely, in the *Wt1*⁺ ovary-derived cell populations, genes involved in growth and proliferation were more enriched along with estrogen receptor 1 (*Esr1*). The major

significance of the two progenitor populations is that they are able to differentiate into two functional cells and play separate but complementary roles in ovarian function and folliculogenesis. Research surrounding the exact mechanism regulating the origin and differentiation of theca cells is limited and brief. According to this research, though, the process is complex and does not rely on just one factor but a complex network of factors. How these factors regulate the process of theca cell recruitment and differentiation is still widely unknown. Although the specifics remain elusive, the differentiation of theca cells is known to be regulated by the local follicular environment. Theca-granulosa co-culture experiments show that the proliferation of theca cells and steroid hormone secretion can be stimulated by the presence of granulosa cells (Kotsuji et al., 1990; Tajima et al., 2006; Orisaka et al., 2006). The proposed paracrine signaling begins with the granulosa cells secreting the Hedgehog (Hh) ligand, which is responsible for lineage specification in many other species (Varjosalo et al., 2008). Based on studies in *Drosophila*, the Hh pathway was found to mainly consist of the ligand Hh, the receptor patched (PTCH) (Ingham et al., 1991), the intermediate protein smoothed (SMO), (van den Heuvel et al., 1996) and the transcription factor cubitus interruptus (Ci) (Varjosalo et al., 2006). The signaling pathway begins with the presence or absence of Hh if present SMO is activated via its phosphorylation sites, protein kinase A and casein kinase 1 (Apionishev et al., 2005). Then, SMO transmits signals to Ci through the costal-2 (Cos2)-fused (Fu) complex, causing dephosphorylation and release of Ci into the cytoplasm (Ho et al., 2005). When Hh is absent, PTCH inhibits the expression and activity of SMO on the membrane, resulting in the phosphorylation of Ci. The phosphorylation causes its ubiquitination to

form a 75-kD fragment (Ci-75). These fragments accumulate in the cytoplasm and diffuse into the nucleus to inhibit target gene expression (Collins et al., 2005).

1.8 Sonic Hedgehog signaling in the ovary

In an adult ovary Indian hedgehog (*Ihh*) and Desert hedgehog (*Dhh*), homologous genes for the ligand Hh, are detected in the granulosa cells with the downstream targets GLI family zinc finger 1/2 (*Gli1/2*), *PTCH1/2*, huntingtin-interacting protein 1 (*Hip-1*) expressed in the theca cell layer (Wijgerde et al., 2005; Liu et al., 2015). Expression of *Ihh* and *Dhh* and their downstream targets *Ptch1*, *Gli1*, and *Gli2* is absent in the fetal mouse ovary (Yao et al., 2002). In mice, a specific knockout of *Dhh* or *Ihh* in granulosa cells led to a significant decrease in the expression of the steroidogenic genes *Cyp17a1* and *Star*, as well as a disruption in the formation of theca cells and antral follicle formation (Lui et al., 2015). In another layer of regulation, the oocyte itself secretes GDF-9, which impacts the expression of *Dhh* and *Ihh*, which has an impact on *Ptch1*, creating a nuanced regulatory network (Lui et al., 2015). The SMO protein is a seven-transmembrane signal transduction protein that is located in the cell membrane and works as a connection that links PTCH and Gli. When *Smo* is overexpressed, mice are found to be infertile, unable to ovulate, and lacking smooth muscle in the follicles. More specifically, they found that platelet endothelial cell adhesion molecule (PECAM) density was increased in the cortex, and vascular support cells were insufficient in the theca layers (Ren et al., 2012). Throughout the ovulation process, vasoconstriction of the follicular vessels is essential for follicle rupture and successful ovulation (Migone et al., 2016). Though the process is critical for competent follicle development, the process of theca cell recruitment has been largely neglected. Deeply understanding how these signaling pathways communicate to

ensure follicle success is critical for in vitro follicle culture and understanding how to navigate ovarian follicle failures.

This comprehensive literature review provides a detailed exploration of various aspects of ovarian biology, focusing on the importance of stromal cells, the development of ovarian follicles, and the regulation of theca cell recruitment in the context of the estrous cycle. Importantly, the review emphasizes the often-overlooked stromal cells within the ovary, describing their role in extracellular matrix deposition and highlighting their potential importance in ovarian function. It discusses the recruitment of theca cells into the follicular unit, exploring theories about the origin and differentiation of these cells, as well as the role of Sonic Hedgehog signaling in regulating this process.

Overall, this literature review provides a comprehensive overview of ovarian biology, shedding light on the complexities of follicle development, stromal cell involvement, and theca cell recruitment. It underscores the need for further research in these areas to advance our understanding of ovarian function and its implications for assisted reproduction.

1.9 References

- Achvarova R, Cohen EM, De Leon V, Tokunaga K, Sakiyama S, Paynton BV 1989 Amounts and modulation of actin mRNAs in mouse oocytes and embryos. *Development* 106:561-565
- Adhikari D, Flohr G, Gorre N, Shen Y, Yang H, Lundin E, Lan Z, Gambello MJ, Liu K 2009 Disruption of Tsc2 in oocytes leads to overactivation of the entire pool of primordial follicles. *Mol Hum Reprod* 15:765-770
- Albertini DF, Combelles CM, Benecchi E, Carabatsos MJ 2001 Cellular basis for paracrine regulation of ovarian follicle development. *Reproduction* 121:647-653
- Apionishev S, Katanayeva NM, Marks SA, Kalderon D, Tomlinson A. Drosophila smoothed phosphorylation sites essential for hedgehog signal transduction. *Nat Cell Biol* 2005;7:86-92. doi: <https://doi.org/10.1038/ncb1210>.
- Bruzzone R, White TW, Paul DL 1996 Connections with connexins: the molecular basis of direct intercellular signaling. *Eur J Biochem* 238:1-27
- Castrillon DH, Miao L, Kollipara R, Horner JW, DePinho RA 2003 Suppression of ovarian follicle activation in mice by the transcription factor Foxo3a. *Science* 301:215-218
- Centers for Disease Control and Prevention. (n.d.). What is assisted reproductive technology (ART)? Retrieved from <https://www.cdc.gov/art/whatis.html>
- Collins RT, Cohen SM. A genetic screen in *Drosophila* for identifying novel components of the hedgehog signaling pathway. *Genetics* 2005;170:173-184. doi: <https://doi.org/10.1534/genetics.104.039420>.
- Edwards RG 1974 Follicular fluid. *J Reprod Fertil* 37:189-219
- Erickson GF, Magoffin DA, Dyer CA, Hofeditz C 1985 The ovarian androgen producing cells: a review of structure/function relationships. *Endocr Rev* 6:371-399
- Eppig JJ 1994 Oocyte-somatic cell communication in the ovarian follicles of mammals. *Sem Devel Biol* 5:51-59

Ghersevich SA, Poutanen MH, Martikainen HK, Vihko RK 1994 Expression of 17 beta-hydroxysteroid dehydrogenase in human granulosa cells: correlation with follicular size, cytochrome P450 aromatase activity and oestradiol production. *J Endocrinol* 143:139-150

Gonzalez-Robayna IJ, Falender AE, Ochsner S, Firestone GL, Richards JS 2000 Follicle-Stimulating hormone (FSH) stimulates phosphorylation and activation of protein kinase B (PKB/Akt) and serum and glucocorticoid-Induced kinase (Sgk): evidence for A kinase-independent signaling by FSH in granulosa cells. *Mol Endocrinol* 14:1283-1300

Ho KS, Suyama K, Fish M, Scott MP. Differential regulation of hedgehog target gene transcription by Costal2 and suppressor of fused. *Development* 2005;132:1401-1412. doi: <https://doi.org/10.1242/dev.01689>.

Holt JE, Jackson A, Roman SD, Aitken RJ, Koopman P, McLaughlin EA 2006 CXCR4/SDF1 interaction inhibits the primordial to primary follicle transition in the neonatal mouse ovary. *Dev Biol* 293:449-460

Hatzirodos N, Hummitzsch K, Irving-Rodgers HF, Rodgers RJ. Transcriptome profiling of the theca interna in transition from small to large antral ovarian follicles. *PLoS One* 2014;9:e97489. doi: <https://doi.org/10.1371/journal.pone.0097489>.

Kotsuji F, Kamitani N, Goto K, Tominaga T. Bovine theca and granulosa cell interactions modulate their growth, morphology, and function. *Biol Reprod* 1990;43:726-732. doi: <https://doi.org/10.1095/biolreprod43.5.726>.

Ingham PW, Taylor AM, Nakano Y. Role of the *Drosophila* patched gene in positional signalling. *Nature* 1991;353:184-187. doi: <https://doi.org/10.1038/353184a0>.

Irving-Rodgers HF, van Wezel IL, Mussard ML, Kinder JE, Rodgers RJ. Atresia revisited: two basic patterns of atresia of bovine antral follicles. *Reproduction* 2001;122:761-775. doi: <https://doi.org/10.1530/rep.0.1220761>.

Migone FF, Cowan RG, Williams RM, Gorse KJ, Zipfel WR, Quirk SM. In vivo imaging reveals an essential role of vasoconstriction in rupture of the ovarian follicle at ovulation.

Proc Natl Acad Sci U S A 2016;113:2294-2299. doi: <https://doi.org/10.1073/pnas.1512304113>.

Oktay K, Briggs D, Gosden RG 1997 Ontogeny of follicle-stimulating hormone receptor gene expression in isolated human ovarian follicles. *J Clin Endocrinol Metab* 82:3748-3751

Orisaka M, Tajima K, Mizutani T, Miyamoto K, Tsang BK, Fukuda S, et al. Granulosa cells promote differentiation of cortical stromal cells into theca cells in the bovine ovary. *Biol Reprod* 2006;75:734-740. doi: <https://doi.org/10.1095/biolreprod.105.050344>.

Reddy P, Liu L, Adhikari D, Jagarlamudi K, Rajareddy S, Shen Y, Du C, Tang W, Hamalainen T, Peng SL, Lan ZJ, Cooney AJ, Huhtaniemi I, Liu K 2008 Oocyte-specific deletion of Pten causes premature activation of the primordial follicle pool. *Science* 319:611-613

Reeves G 1971 Specific stroma in the cortex and medulla of the ovary. Cell types and vascular supply in relation to follicular apparatus and ovulation. *Obstetrics and Gynecology* 37 832–844. (<https://doi.org/10.1097/00006254-197203000-00016>)

Ren Y, Cowan RG, Migone FF, Quirk SM. Overactivation of hedgehog signaling alters development of the ovarian vasculature in mice. *Biol Reprod* 2012;86:174. doi: <https://doi.org/10.1095/biolreprod.112.099176>.

Richards JS, Ren YA, Candelaria N, Adams JE, Rajkovic A. Ovarian follicular theca cell recruitment, differentiation, and impact on fertility: 2017 update. *Endocr Rev* 2018;39:1-20. doi: <https://doi.org/10.1210/er.2017-00164>.

Varjosalo, M. & Taipale, J. Hedgehog: functions and mechanisms. *Genes Dev.* **22**, 2454–2472 (2008).

Sawetawan C, Milewich L, Word RA, Carr BR, Rainey WE 1994 Compartmentalization of type I 17 beta-hydroxysteroid oxidoreductase in the human ovary. *Mol Cell Endocrinol* 99:161-168

Simoni M, Gromoll J, Nieschlag E 1997 The follicle-stimulating hormone receptor: biochemistry, molecular biology, physiology, and pathophysiology. *Endocr Rev* 18:739-773

Simon AM, Goodenough DA, Li E, Paul DL 1997 Female infertility in mice lacking connexin 37. *Nature* 385:525-529

Sullivan SD, Castrillon DH 2011 Insights into primary ovarian insufficiency through genetically engineered mouse models. *Semin Reprod Med* 29:2890-2894

Tajima K, Orisaka M, Yata H, Goto K, Hosokawa K, Kotsuji F. Role of granulosa and theca cell interactions in ovarian follicular maturation. *Microsc Res Tech* 2006;69:450-458. doi: <https://doi.org/10.1002/jemt.20304>.

Wijgerde, M., Ooms, M., Hoogerbrugge, J. W. & Grootegoed, J. A. Hedgehog signaling in mouse ovary: Indian hedgehog and desert hedgehog from granulosa cells induce target gene expression in developing theca cells. *Endocrinology* **146**, 3558–3566 (2005).

Yao HH, Whoriskey W, Capel B. Desert hedgehog/patched 1 signaling specifies fetal Leydig cell fate in testis organogenesis. *Genes Dev* 2002;16:1433-1440. doi: <https://doi.org/10.1101/gad.981202>.

Young JM, McNeilly AS. Theca: the forgotten cell of the ovarian follicle. *Reproduction* 2010;140:489-504. doi: <https://doi.org/10.1530/REP-10-0094>.

Yamamoto S, Konishi I, Tsuruta Y, Nanbu K, Mandai M, Kuroda H, et al. Expression of vascular endothelial growth factor (VEGF) during folliculogenesis and corpus luteum formation in the human ovary. *Gynecol Endocrinol* 1997;11:371-381. doi: <https://doi.org/10.3109/09513599709152564>.

Zhang Y, Word RA, Fesmire S, Carr BR, Rainey WE 1996 Human ovarian expression of 17 beta-hydroxysteroid dehydrogenase types 1, 2, and 3. *J Clin Endocrinol Metab* 81:3594-3598

CHAPTER 2. SINGLE CELL RNA SEQUENCING OF THE BOVINE OVARY

2.2 Introduction

The intricate processes and multifaceted functions of the ovary have captivated researchers for decades, driving an extensive body of literature that attempts to unravel the complexities of ovarian biology. However, despite many major breakthroughs, there are still significant gaps in our knowledge about the cell populations that make up the ovary. The follicle is considered the functional unit within the ovary and is typically the focus of most research whereas most of the remaining cells present reside under the umbrella of “stromal” cells. This umbrella typically includes immune cells, blood vessels, nerves, lymphatic vessels, and uncharacterized cells. In addition to these general components, other ovarian cells such as ovarian surface epithelium, tunica albuginea, intraovarian rete ovarii, hilar cells can sometimes be included in the stromal group (Shikanov et al., 2020). The specific roles of each cell type are only partially understood. Immune cell presence fluctuates over the course of the estrous cycle and increases during the development of the corpus luteum (Normal et al., 1994). Specifically, macrophages are a predominant immune cell type in the ovary, with others at a lesser amount including B and T lymphocytes, natural killer cells, dendritic cells, neutrophils, eosinophils, and mast cells (Norman et al., 1994, Suzuki et al., 1998, Carlock et al., 2013, Kenngott et al., 2016, Fan et al., 2019, Zhang et al., 2020). The uncharacterized group of stromal cells is a heterogeneous population and includes cells described as fibroblast-like, spindle-shaped, or interstitial cells (Reeves 1971). In general, fibroblasts are

responsible for synthesis of extracellular matrix (ECM) proteins such as collagen for cellular support, scaffolding and repair (Berkholtz et al., 2006). The descriptions that have been used to characterize the ovarian stromal populations and, more specifically, fibroblast-like, spindle-shaped, and interstitial cells are limited and only describe their general morphology. Overall, a specific description of the stromal population, including specific markers that could shed light on cell function, remains scarce. Emerging technologies such as single-cell RNA sequencing (scRNAseq) provide insight into what subtypes exist within the ovarian stroma and their potential role in ovarian function. Single cell RNA sequencing has led to the characterization of the human follicle, and identifying stem cell progenitors in *Drosophila* (Fan et al., 2019; Morris et al., 2022; Slaidina et al., 2020).

Studies in *Drosophila melanogaster* led to the identification of the Hedgehog (Hh) gene (Nusslein-Volhard et al., 1980). Following this, three vertebrate homologs of Hh have been identified: Sonic hedgehog (Shh), Indian hedgehog (Ihh), and Desert hedgehog (Dhh) (Echelard et al., 1993; Krauss et al., 1993; Riddle et al., 1993; Chang et al., 1994). In the mouse ovary, the ligands Ihh and Dhh are found exclusively in the granulosa cells of the growing follicles and communicate through paracrine signaling to activate the hedgehog cell surface receptors PATCHED 1 and 2 (PTCH1 and PTCH2) located in the pre-theca or stromal surrounding cells (Wijgerde et al., 2005; Ren et al., 2009; Ren et al., 2012; Spicer et al., 2009). Activation of PTCH1/2 releases the inhibition of the G protein-like receptor Smoothed (SMO), leading to the nuclear translocation of the transcription factors glioma-associated oncogene homolog 1 and 2 (GLI1 and GLI2) (Liu et al., 2015; Wijgerde et al., 2005; Russell et al., 2007). The localized expression of GLI1 and GLI2

near the follicle but not directly within the theca layer has led these factors to be postulated as putative markers of theca-precursor cells. When comparing mRNA expression levels from large and small follicles in the bovine, *PTCH1* and *SMO* are significantly higher in theca cells in large when compared to small follicles (Spicer et al., 2009). Additionally, *Ihh* is significantly expressed at higher levels in the granulosa cells of the smaller follicles supporting the current proposed mechanism of theca cell recruitment (Spicer et al., 2009).

Here, we used single cell RNA sequencing (scRNAseq) in a first attempt to characterize the different cell populations present in the bovine ovarian cortex, and particularly the stromal cell population, based on their individual gene expression pattern. Our hypothesis was that distinct cell types could be identified within the ovarian stroma using individual cell signature. We determined three distinct subtypes of cells within the ovarian stroma, whose gene expression profiles suggest distinct remodeling functions. Using immunohistochemistry, we confirmed the localization of collagens IV and V observed in scRNAseq to different regions of the ovary, indicating a more specific organizational structure than previously thought.

2.2 MATERIALS AND METHODS

All materials were purchased from Thermo Fisher Scientific unless otherwise specified.

2.2.1 Optimization of ovarian tissue dissociation to maximize viability in single cell suspensions.

The bovine ovarian cortex is a fibrous and dense tissue. Therefore, the first step was to establish a protocol to maximize the viability of single cells obtained from frozen-thawed tissue, at the same time minimizing debris that could interfere with downstream

applications. The original dissociation protocol was a modified version of the mouse ovarian dissociation described by Tilly et al., 2013. Briefly, the amount of collagenase type IV was increased to 1 mg/mL, liberase was added at a concentration of 50 µg/mL, serological pipetting time was increased to improve cell dissociation, and addition of a filtration step through a 30 µm cell strainer after each wash and after centrifugation.

2.2.2 Tissue Dissociation for single cell sequencing

Two nuliparous heifers 49-52 days pregnant were euthanized, and all four their ovaries were harvested and immediately taken to the laboratory. The ovarian cortex was dissected from the ovarian ligament and medulla and 300 mg fragments of cortical tissue were isolated and placed in a cryovial containing 1 mL of 1.5 M of dimethyl sulfoxide (DMSO), and 15% (150µL/1mL) fetal bovine serum (FBS) in minimal essential media (MEM) (Gibco, Waltham, Massachusetts, USA). The cryovials were placed in a slow freezing instrument (Cryologic, Blackburn, Australia) to equilibrate at 20°C for 20 min and then chilled at 0.3 °C/min until -38 °C and then moved to LN2 for long term storage. For thawing, the cryovial was placed on a bead bath at 38°C until there was still a large ice chunk in the tube. The tissue was then removed and moved through a wash sequence using a 6-well plate containing MEM media at room temperature, 5 min in each well. Each tissue piece was then minced using scissors into a 50 mL conical tube containing 1mg/mL of collagenase type IV, 50 mg/mL of Liberase, and 1 U/ml DNase I, within 10 mL of Hanks Balanced Salt Solution with Calcium and Magnesium (HBSS^{+/+}). This enzyme cocktail was prewarmed to 38 °C prior to beginning dissociation. The tissue was completely minced and then incubated on an orbital shaker at 38°C for 10 min. The tissue was then pipetted up and down (15 times at least) using a 5 mL serological pipette and put back

on the orbital shaker for an additional 10 min. The remaining tissue was pipetted up and down again using a 5 mL serological pipette. The enzymes were inhibited with 5% FBS and then filtered through a 70 μm filter and a 30 μm filter. The filter and tube were rinsed using HBSS without calcium and magnesium. Prior to centrifugation, the centrifuge was set to 8°C and allowed to cool ahead of time, and the cells were centrifuged at 700 x g for 5 min at 9 acceleration and no brake. The following steps were performed on ice to help maintain cell viability. The cells were filtered once more through a 30 μm filter and then resuspended in 2 mL of cold HBSS^{-/-} counted, and viability was determined using a hemocytometer and Trypan blue. Cell viability was 70% or greater before submission. Figure 1 depicts the steps starting with the obtention of ovarian cortical fragments until submission of single-cell suspensions for sequencing (Fig. 1A) and details of the 10x Chromium platform for scRNAseq (Fig. 1B).

2.2.3 scRNAseq and data preprocessing

Single-cell suspensions were submitted to the DNA Technologies core at the University of California's Genome Center for scRNAseq. Each sample had a concentration of single cells in suspension of 1×10^3 cells/ μl in a volume of 500 microliters. Cells were loaded according to the standard protocol of the Chromium single-cell 3' reagent kit (10x Genomics; Pleasanton, CA) to capture 5,000 to 10,000 cells/chip position (V3 chemistry). The microfluidic design of the chip allows for each individual cell to be paired with one gel bead that contains the barcoded oligonucleotide. Then the single cells are lysed, the gel beads are dissolved to free the barcoded oligonucleotides into solution, and reverse transcription of polyadenylated mRNA occurs. As a result, all cDNAs from a single cell will have the same barcode, allowing the sequencing reads to be mapped back to their

original single cell of origin. The preparation of next-generation sequencing libraries from these barcoded cDNAs is then carried out in a bulk reaction.

Library preparation was performed according to instructions in the 10× Genomics Chromium platform. The libraries were then pooled and sequenced on an Illumina NovaSeq 6000 System. Reads were processed using the Cell Ranger 3.0.1 pipeline (<https://support.10xgenomics.com>) with default, recommended parameters. The cell ranger pipeline was used to demultiplex the data as well as generate feature-barcode matrices. The raw sequence files were aligned to the bovine reference genome with the STAR algorithm (Dobin et al., 2013). Finally, a gene–barcode multi-dimensional matrix containing the barcoded cells and gene expression counts was generated.

2.2.4 Data analysis

The RStudio (Boston, Massachusetts, USA) software package Seurat was used for further analysis. The barcode matrix was processed with Seurat v3 (Butler et al., 2018), a toolkit for scRNA-seq data analysis. All functions were run using default parameters unless otherwise specified. Low-quality cells (<300 genes/cells, <3 cells/gene, and >20% mitochondrial genes) were excluded. Then, the Unique Molecular Identifiers (UMI) count data were normalized with log transformation. The highly variable genes (HVGs) were selected to amalgamate samples into a merged data set. Next, the merged cell-by-gene matrix was scaled by dividing the centered expression by the standard deviation. Counts were normalized using the default normalization approach of Seurat (Function NormalizeData). Briefly, for each cell, the UMI counts for each gene were divided by the

sum of UMI counts for all genes for that cell. The result was multiplied by a fixed factor (10,000) and log-transformed.

After log transformation, prior to clustering, genes associated with the cell cycle were analyzed, and if they contributed to differences in clustering, they would be regressed out of the data (Stuart et al., 2019). Cell cycle phase scores were calculated based off of canonical markers and scoring strategy used by Tirosh et al., 2016. If the cell cycle is heterogenous confounding the clustering analysis, the expression of genes related to the cell cycle is scaled to represent a “corrected” expression matrix. In the case of this dataset, cell cycle related genes did not affect clustering analysis therefore, no changes were made. A principal component analysis of the most variable genes was performed, and an elbow plot was used to select the principal components that captured the most variance within the dataset. These principal components were used as edge weights in an unsupervised graph-based clustering to identify cell clusters following the Seurat analysis pipeline. A uniform manifold approximation and projection (UMAP) was generated for visualization of the cell clusters. Expression levels of cell-type specific markers were used to determine the putative identities for each cell cluster.

2.2.5 Cluster Identification

Once the number of clusters in the samples was defined based on the elbow plot, the FindAllMarkers function was used to determine the major differentially expressed genes in each cluster using a Wilcoxon rank sum test, where the adjusted p-value, based on Bonferroni correction using all features in the dataset was $P_{adj} < 0.05$. Following that, the Extract_Top_Markers was utilized to narrow this to the top 5 markers per cluster for

further analysis. Using these top 5 markers, a clustered dotplot was formed to provide clarity for each cell cluster and their most differentially expressed genes. Those gene expression profiles were used to determine the cell types.

2.2.6 Sub clustering Analysis

Following the steps described above, the stromal cell population was determined using the expression of *COL1A1* and *COL6A1*, which encode the proteins collagen I and VI. Then, the FindSubCluster function of Seurat was used to determine the most variable clusters of cells within the stromal population (Stuart et al., 2019). A total of three subclusters were identified, and the most differentially expressed genes in these clusters were then put into Ingenuity Pathway Analysis (Qiagen, Venlo, The Netherlands) to determine biological functions and molecular and cellular components.

2.2.7 Preparation of ovarian tissue for immunohistochemical analysis

Upon harvest, fragments of ovarian cortex from each heifer were dissected. These pieces were fixed in 10% neutral buffered formalin for 24 hours and then placed in a 30% sucrose solution for 48 hours before embedding in optimal cutting temperature compound (O.C.T.), frozen at -80 °C, sectioned with a cryostat, and mounted onto positively charged glass slides. Each section was 14 µm thick. Slides containing the sections were kept at -20°C until staining. Prior to immunostaining, the slides were left at room temperature for approximately 20 minutes. Then they were subjected to antigen retrieval by incubating in citric acid antigen unmasking solution at pH 6 (Vector Laboratories, Newark, CA) once it reached 97 °C for 5 min in an uncovered jar, and then let cool to room temperature. The slides were washed with tris buffered saline solution (TBS) and then incubated in a

blocking solution of 1% (50 mg/6 mL) BSA, 10% (500 μ L/mL) Normal Donkey Serum, and 0.3 mM of glycine for one hour to minimize non-specific binding. Next, the slides were incubated with primary antibodies [rabbit polyclonal anti-human collagen IV (ab6586) and rabbit polyclonal anti-human collagen V (ab7046); Abcam; Cambridge, MA] at 1:300 dilution for 18 hours. These antibodies are designed to not cross-react with each other. Next, samples were incubated with a donkey anti-rabbit secondary antibody at a 1:200 dilution for 1 hour. The final step was the incubation in Vector NovaRed (Vector Laboratories, Newark, CA) solution for 15 min before stopping the reaction with the addition of double distilled water. Each animal had a total of 40 sections analyzed/collagen type/animal. In each run of immunostaining, one section was used as a negative control by replacing the primary antibody with a rabbit isotype IgG.

2.2.8 Immunohistochemical Quantification

Qupath software was used for image analysis. Three areas of the cortex were measured in each section: epithelium, tunica albuginea, and perifollicular stroma. Prior to image analysis, a threshold was set for the level of signal that would be considered positive, and what would be considered negative. The threshold was offset based on very positively stained tissue (positive) and part of the tissue that had the least amount of staining (negative). Regions of interest (ROI) were drawn for the epithelium, tunica albuginea (TA), and perifollicular region of the cortex; then QuPath calculated the number of positive pixels per area analyzed as a percentage of the total area of that ROI. The perifollicular areas were measured by drawing two squares immediately around each follicle; the percentage of positive pixels was calculated for each square and then averaged. The epithelium and TA were measured in their totality within each section evaluated,

therefore, each section had only one measurement. This analysis was performed for both collagen IV and collagen V.

2.2.9 Statistical analysis of collagen intensity

The mean proportion of positive pixels per region was analyzed via analysis of variance using SAS software version 9.4 (SAS Institute, Cary, NC). Differences in the proportion of positive pixels were considered significant if the comparisons were associated with $P < 0.05$.

2.3 Results

2.3.1 Major cell types identified in the ovarian cortex based on single cell transcriptome.

Nine clusters were identified in the analysis of gene expression profile: stromal (23%), blood vessels (endothelial 15%, platelets 12%, smooth muscle 2%), lymphatic (13%), immune (myeloid 9%, T-cells 8%, B-Cells 0.3%), granulosa (9%), theca (7%), epithelial (6%), adipocytes (4%), plasma cells (1.2%) (Fig.1).

One of the main goals of this experiment was to gain insight into the cell types that make up the ovarian stromal population. After the initial clustering that defined that the stroma made approximately 23% of the cells in the cortex, we re-clustered this population to magnify the differences between the cells. This reclustering generated three subpopulations, namely extracellular matrix building, vasculature formation, and cell migration clusters. These cell clusters were determined based on their most abundantly expressed genes (Fig.2). The top transcripts in the extracellular matrix forming cluster were *keratin 18 (KRT18)*, *ankyrin repeat domain 1 (ANKRD1)*, ENSBTA00000052369,

ENSBTA00000052756, and ENSBTA00000052187. The top transcripts in the vascular formation cluster were *SPARC-like 1 (SPARCL1)*, *tropomyosin 2 (TPM2)*, *actin alpha 2 (ACTA2)*, and *C-X-C motif chemokine ligand 12 (CXCL12)*. The top transcripts in the cell migration cluster were *multimerin 1 (MMRN1)*, *fatty acid binding protein 5 (FABP5)*, *EGF-like domain multiple 7 (EGFL7)*, *S100 calcium-binding protein A1*, and *C-C motif chemokine ligand 21 (CCL21)*. Next, we evaluated the expression and abundance of collagen proteins and fibronectin, the most abundant components of the extracellular matrix, in each of the clusters (Fig. 3). We observed that collagen I and III were abundant in the ECM building and vasculature formation clusters, and to a lesser extent, in the cell migration cluster. Collagen IV, V, VI, and fibronectin were more abundant in the ECM building cluster compared to the other two. It is worth noting that collagens I, II, IV, and VI have been previously described in the ovary (Lind et al., 2009), whereas to our knowledge, collagen V has not been described before this report. Based on the greater expression of collagen IV and V in the extracellular matrix-building population compared to the other two, we sought to identify this cluster based on protein expression using immunohistochemistry (IHC). We analyzed three distinct areas of the cortex for the presence and abundance of collagen IV and V: the epithelium, perifollicular, and the tunica albuginea. The content of both collagens IV and V was greatest in the epithelium, followed by the tunica albuginea. The perifollicular region had the lowest abundance of both types of collagen (Fig. 4).

2.3.2 Localization of transcripts of the Hedgehog signaling pathway in the bovine ovarian cortex.

We used markers for granulosa (*FSHR*, *FST*, *AMH*, *INHA*) and theca cells (*CYP11A1*) to confirm cluster identity; we then investigated whether transcripts for hedgehog signaling would be represented in these cell populations. Notably (Fig.2) we found expression of *IHH* in a small proportion (0.6%) of the granulosa cells although the level of expression of the transcript in those cells was high (Fig.2). Accordingly, transcripts for *PTCH1* (6.9%), *SMO* (8.1%), *GLI* (1.4%), *HHIP* (2.0%), and *TCF21* (8.3%) were expressed in the theca cell cluster, confirming previous reports that ligands for HH signaling are expressed in granulosa cells, while receptors and downstream signaling molecules are expressed in theca cells.

2.4 Discussion

Recapitulating the ovary *in vitro* has become a much more attainable goal for the foreseeable future, and fully understanding the nuanced cell populations that support follicle growth and hormone production will be essential for an accurate recapitulation. A few research groups have taken interest in the ovarian stroma over the years (Reeves et al., 1971; Kinnear et al., 2020; Berkholtz et al., 2006; Hummitzsch et al., 2019). The ovarian stroma consists of various general components, including immune cells (Wu et al., 2004), blood vessels (Reeves, 1971), nerves (Neilson et al., 1970), and lymphatic vessels (Brown et al., 2010), alongside ovary-specific components. These ovary-specific components comprise the ovarian surface epithelium (Auersperg et al., 2001), tunica albuginea (Reeves, 1971), intraovarian rete ovarii (Wenzel & Odend'hal, 1985), hilar cells (Neilson et al., 1970), ovarian stem cells (Hummitzsch et al., 2015), and stromal cells that have been partially characterized including fibroblast-like, spindle-shaped, and interstitial cells (Reeves, 1971). Additionally, the ovarian extracellular matrix (ECM) plays a vital role

by providing structural and biochemical support to the surrounding cells, serving as a key non-cellular component of the stroma (Berkholtz et al., 2006). Some studies have used broad terms such as 'ovarian interstitial stroma' or 'theca interstitial cells' (TICs) to refer to the heterogeneous stromal compartment (Tingen et al., 2011; Hummitzsch et al., 2019). Our scRNA-seq results confirm that there are different types of stromal cells within the ovary; moreover, their transcript expression profiles suggest unique functions.

By sub clustering the population initially defined as stromal cells, we identified three distinct subpopulations. Based on their pattern of transcript expression, these subpopulations were characterized by the likely processes they facilitate and/or participate in: angiogenesis (vasculature building), cell migration, and extracellular matrix remodeling. The angiogenic cluster was characterized by high expression of *SPARC1* (*endothelial tissue marker*), *MGP* (secreted by vascular smooth muscle cells), and *ACTA2* (specific to vasculature contractility) (Nashberger et al., 2021; Aaseth et al., 2020; Stavely et al., 2022). The cell migration cluster showed high level of expression of *EGFL7* (EGF-like domain multiple 7) an epidermal like growth factor domain that plays a role in smooth muscle migration (Stuhlmann et al., 2012). The extracellular matrix building population showed the highest expression of matrix metalloproteinases 2 and 14 (MMP2/14) and tissue inhibitors of metalloproteinases 2 and 3 (TIMP2/3) (Maskos et al., 1999). An interesting observation is was that collagen expression was not ubiquitous throughout the stromal subpopulations. Previous reports have described the presence of collagens I-IV within the extracellular matrix of the ovary. Here, we found that collagen V (*COL5A1*), which has not yet been described in the ovary, was expressed in a variety of cells within the stroma, being particularly abundant in the ECM building cluster. Based on this new

finding, we used IHC to localize and perform a semi-quantitative evaluation of the abundance of collagen IV (known to be abundant in the ovarian cortex) and collagen V (newly identified collagen in the bovine ovary) in relation to a follicular structure and to the surface of the ovary. Our results showed that both collagens are significantly more abundant in the epithelium, followed by the tunica albuginea. In contrast, the perifollicular area of the stroma has the least abundance compared to the other two regions. The less abundant collagen in the perifollicular region is expected, given the need for the tissue to accommodate follicular growth; similarly, the epithelium would be the region where a more effective barrier is critical, and this barrier is provided by collagens. Collagen IV and V localization patterns were similar in the ovarian cortex. Although antibodies chosen bind to unique sequences of each collagen type, the possibility of overlap cannot be discarded, being at least partially caused by a lack of specific binding.

The mechanism governing the recruitment of theca cells into the follicular unit has remained elusive in ovarian biology; however, the hedgehog signaling pathway is believed to play an important role in regulating the origins of theca cells (Wijerde et al., 2005). The hedgehog pathway consists of the ligands Shh, Ihh and Dhh, the receptor patched (PTCH), (Ingham et al., 1991), the intermediate protein smoothed (SMO; (Van den Heuvel et al., 1996), and the transcription factor cubitus interruptus (Ci; Varjosalo et al., 2006). In the mouse, the ligand Indian hedgehog (*Ihh*) has been reported to be expressed within the granulosa cells, while patched 1/2 (*Ptch1/2*), inhibitory decoy receptor Hedgehog interacting protein *Hhip*, and *Gli1*, which function as receptors and downstream signaling molecules, are expressed by the theca cells (Wijerde et al., 2005). We identified in our data that *IHH* was expressed mostly within the granulosa cell cluster.

Although the number of cells expressing *IHH* was low, the expression within those cells was high. This could indicate the existence of a subcluster of granulosa cells responsible for secreting this protein, although further studies are needed to confirm this hypothesis. In the theca cell cluster, we saw the highest expression of *PTCH1*, *GLI1*, and *HHIP*. We also observed expression of *SMO* which is inhibited by *PTCH1* to signal downstream activation of transcription factors. These findings confirm previous reports in mouse (Wijerde et al., 2005) and bovine (Spicer et al., 2009) that the components of HH signaling are present in the granulosa and theca cells. Further mechanistic studies will be critical to determine if hedgehog signaling is, in fact, responsible for theca cell recruitment in the bovine ovary and whether granulosa cells are the ones initiating this process.

As assisted reproduction technologies continue to advance, we must move toward creating in vitro environments that better mimic the native ovary. To accomplish this goal, it is critical that we know the ovary at the single-cell level to ensure the production of healthy oocytes that yield competent embryos and, ultimately, healthy offspring. This is the first report of sequencing of the bovine ovary at the single-cell level. Based on distinct patterns of gene expression by individual cells, we confirmed that the ovary is a complex organ made of specialized somatic cells in addition to the gametes. One of our main goals was to learn more about the ovarian stroma, given that a thorough characterization of this compartment is still missing. The ovarian stroma plays critical roles in providing cells for the follicular unit and providing support for follicle growth and ovulation. Our data show that the stroma is made of multiple cell types, among which we could identify three main groups based on differential gene expression. There is clearly a need to continue to

unravel the subtle differences between cells and how they interact to accomplish the different processes necessary for proper ovarian function.

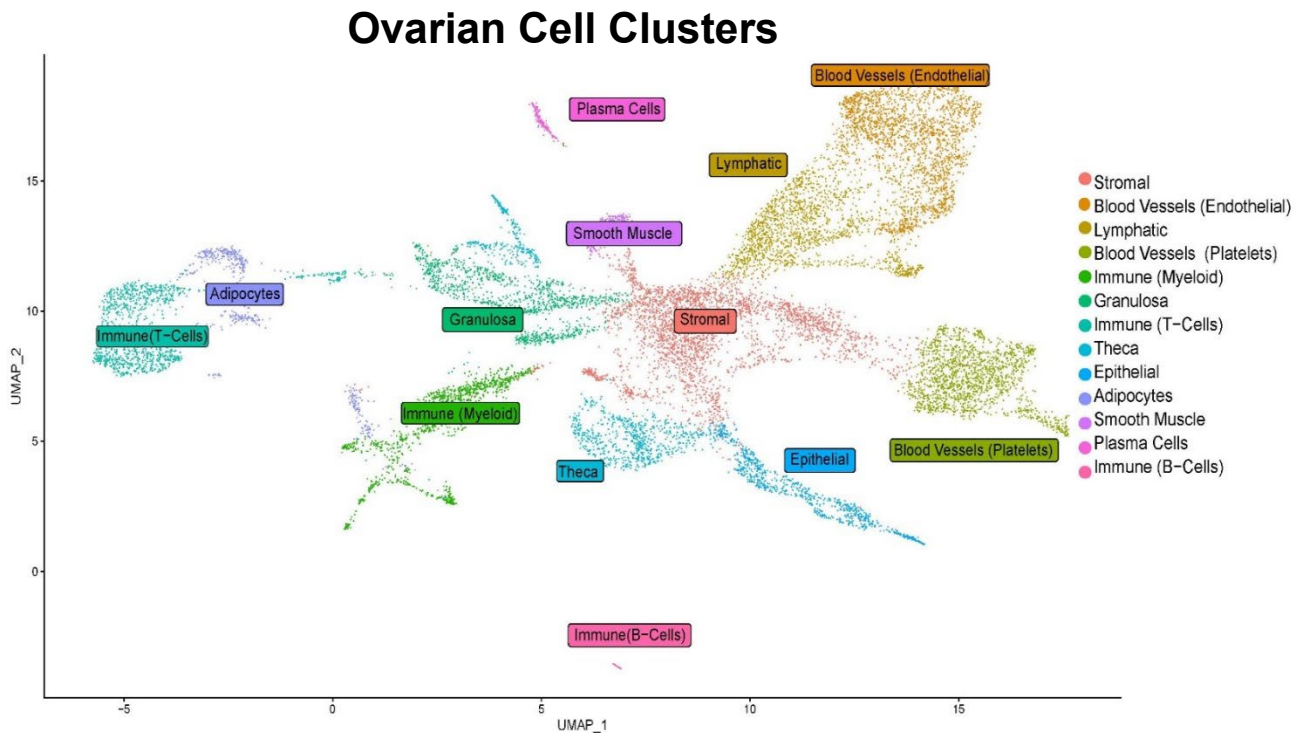
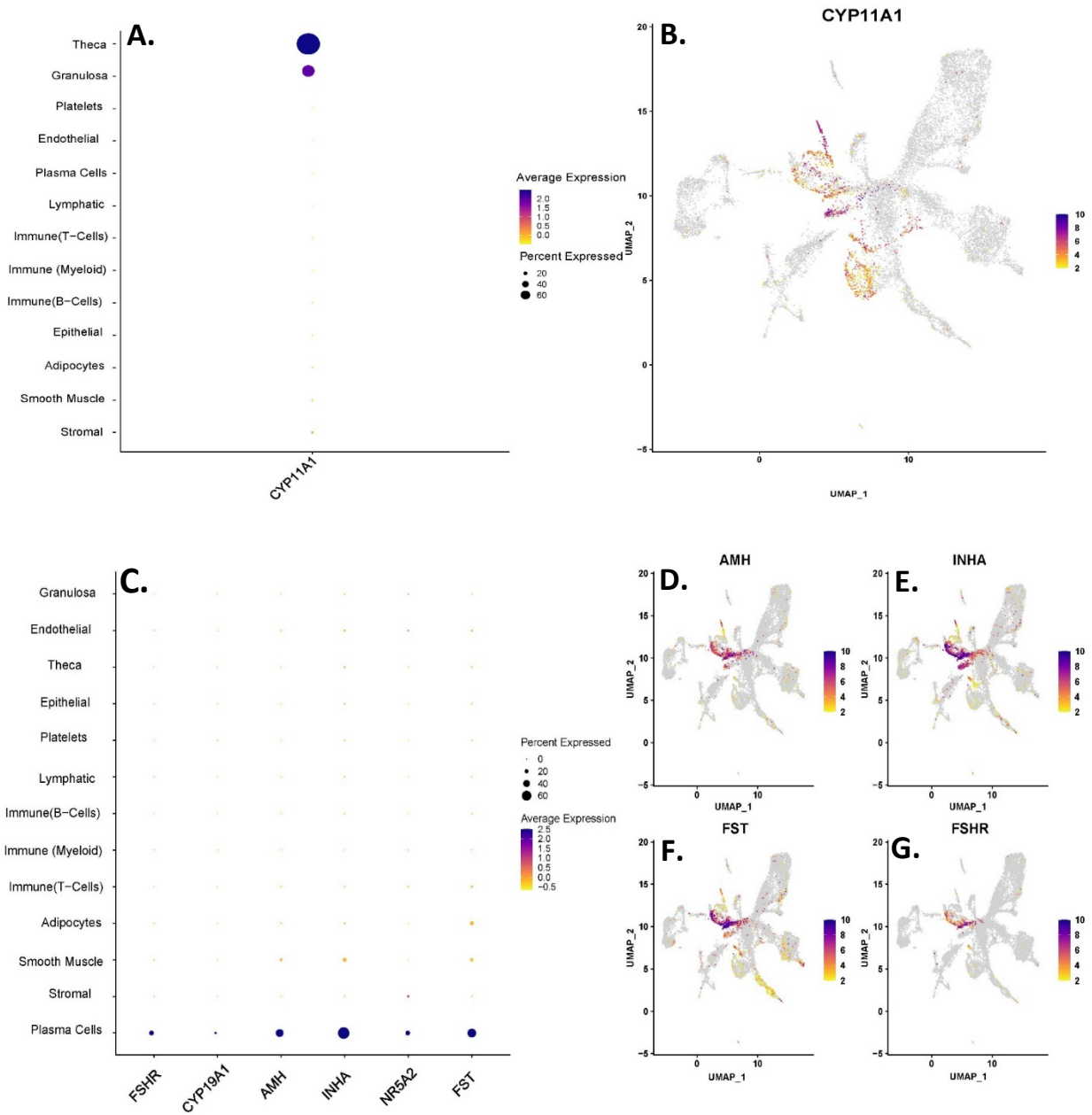


Figure 1. The cell types that are present in the pregnant adult bovine ovary. Cells from two pregnant heifers were isolated and sequenced using 10x genomics. After quality control, filtration, and integration 12,587 cells were analyzed. A uniform manifold approximation and projection (UMAP) plot featuring the different clusters in the ovary.

Ovarian Specific Clusters



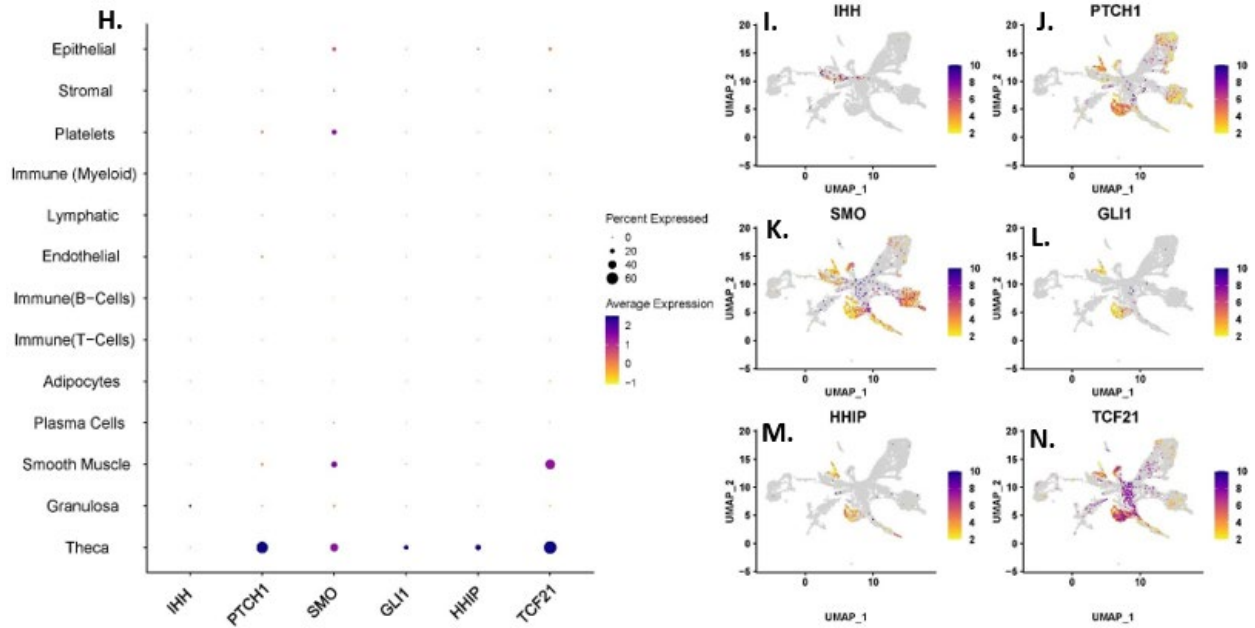
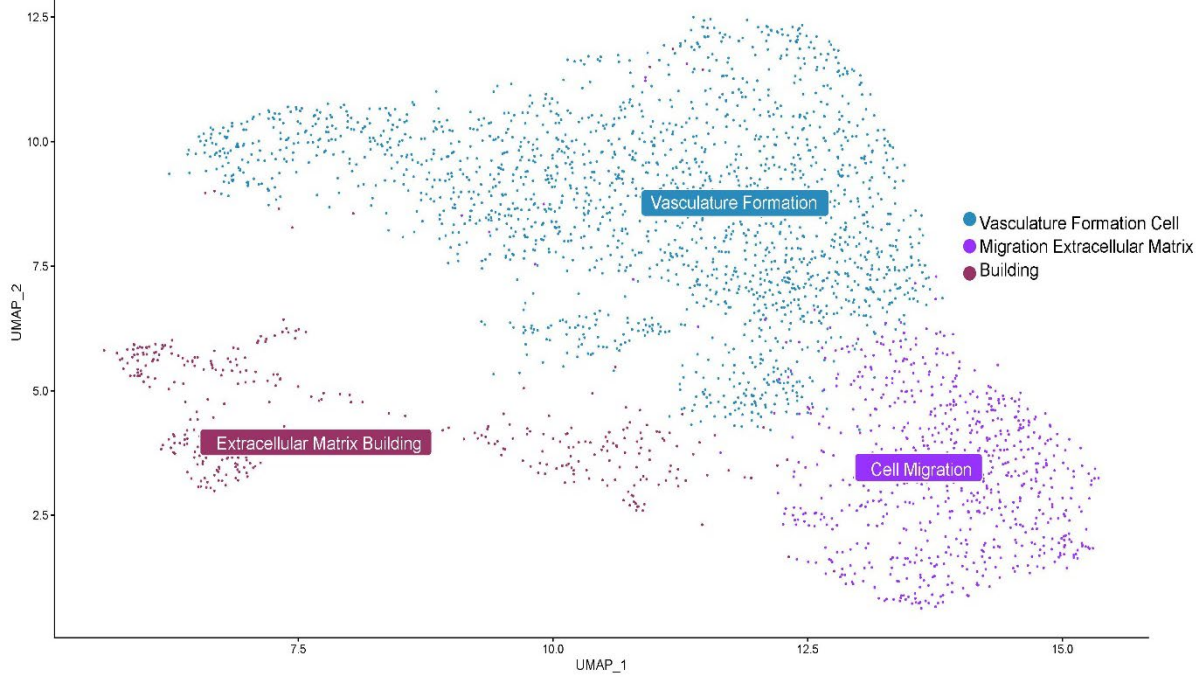


Figure 2. Ovarian Specific clusters; A-B. Showcasing CYP11A1, associated with Theca cells, amount (in the form of a dotplot) as well as the location (in the form of a feature plot) of expression within all the cell clusters. **C-G.** Showcasing granulosa cell markers FSHR, CYP19A1, AMH, INHA, NR5A2, and FST expression levels (in the form of a dotplot) and the location (in the form of a feature plot) within all the cell clusters. **H-N.** Showing the expression levels and locations of genes associated with the sonic hedgehog pathway (IHH, PTCH1, SMO, GLI1, HHIP, TCF21).

Stromal Subclusters

A.



B.

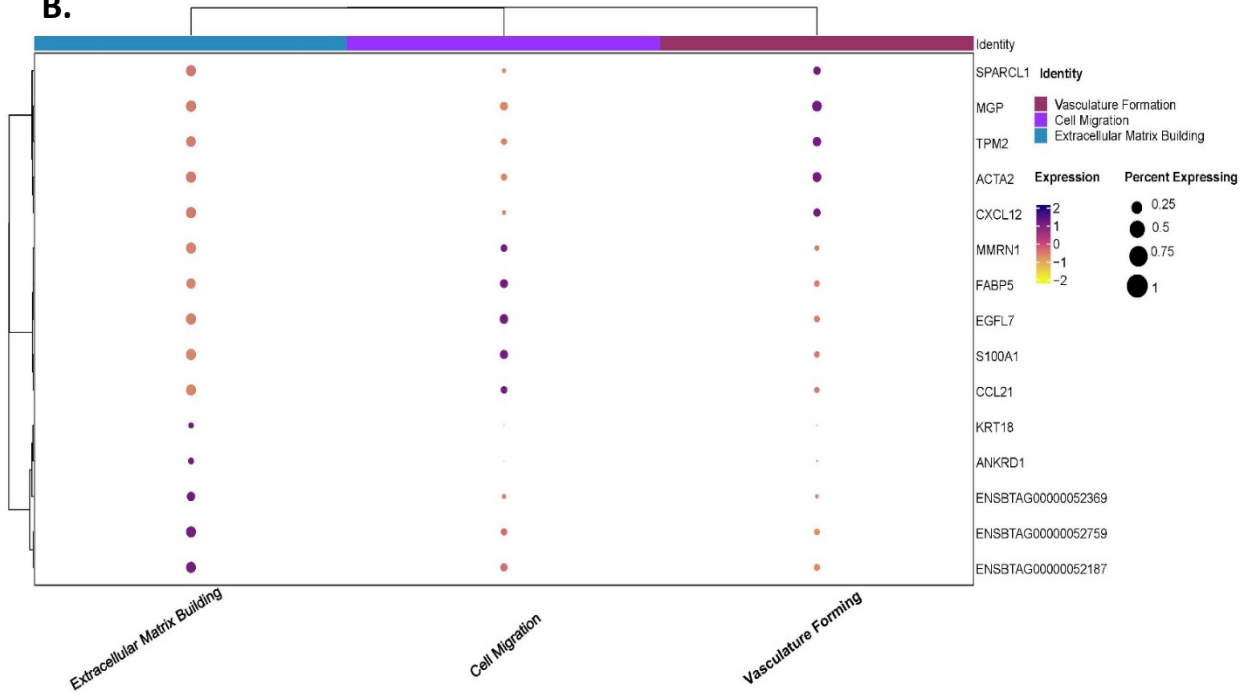


Figure 3. Subpopulations within the Stromal Population. A) A uniform manifold approximation and projection (umap) of the stromal subpopulations. There are three clusters, extracellular matrix building, cell migration, and vasculature forming. These labels are notating the putative functions of these subpopulations within the stroma. B) The top 5 markers determined by pairwise comparisons are shown, with the expression level notated by color and the size noting the percentage of cells expressing that transcript.

Collagen Distribution within the Subclusters

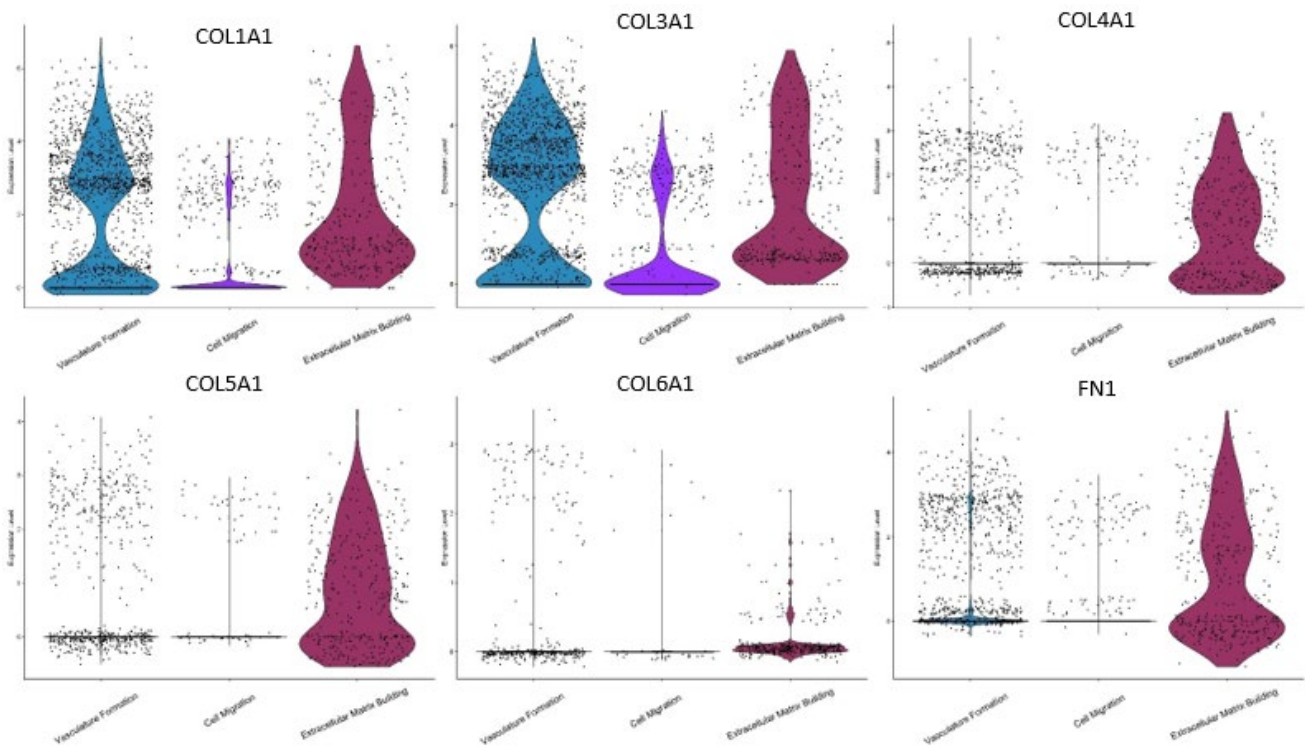


Figure 4. Collagen distribution within the stromal subclusters. Violin plots depicting the expression levels of collagens 1,3-6 and fibronectin.

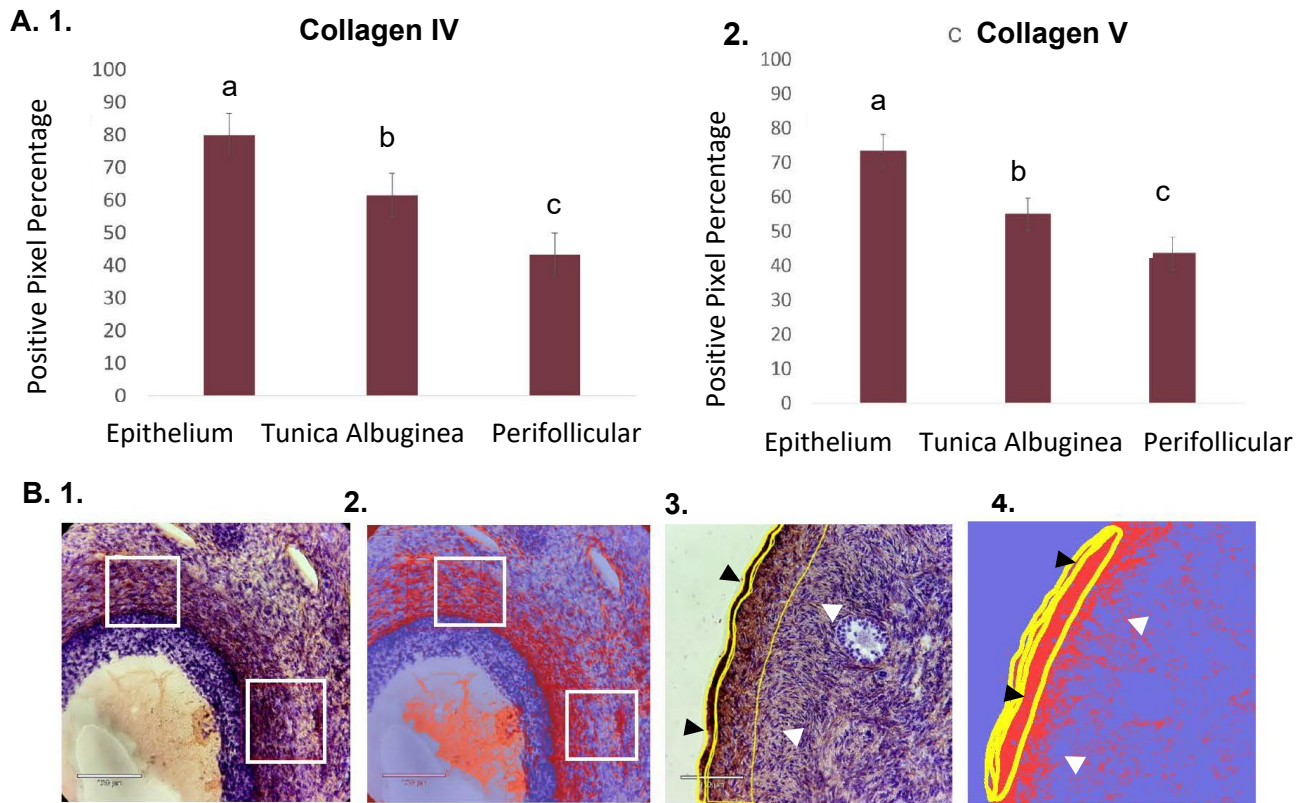


Figure 5. A) Abundance of Collagen IV and V within different regions of the ovarian cortex. Least square means of collagen IV (**A1**) and collagen V (**A2**) in each region evaluated. Overall, both collagen types were more abundant in the epithelium, followed by the tunica albuginea and the perifollicular region surrounding antral follicles. Within each graph, different superscripts indicate significant differences in collagen abundance. **B)** Analysis of Collagen IV and V abundance following IHC. **B)1-2.** Representative image showing one area used for measurement of collagen abundance within the perifollicular region and the pixel measurement of NovaRed positive staining in the same region. **B)3-4** Representative image showing one area used for measurement of collagen abundance within the epithelium (black arrow) and tunica albuginea (white arrowheads) regions and the pixel measurement of NovaRed positive staining in the same regions.

2.5 References

- Bankhead, P. et al. QuPath: Open source software for digital pathology image analysis. *Scientific Reports* (2017). <https://doi.org/10.1038/s41598-017-17204-5>
- Butler A, Hoffman P, Smibert P, Papalexi E, Satija R. Integrating single-cell transcriptomic data across different conditions, technologies, and species. *Nat Biotechnol.* 2018;36:411–20.
- Chang DT, Lopez A, von Kessler DP, Chiang C, Simandl BK, et al. 1994. Products, genetic linkage and limb patterning activity of a murine hedgehog gene. *Development* 120:3339–53
- Dobin A, Davis CA, Schlesinger F, Drenkow J, Zaleski C, Jha S, et al. STAR: ultrafast universal RNA-seq aligner. *Bioinformatics.* 2013;29:15–21.
- Echelard Y, Epstein DJ, St-Jacques B, Shen L, Mohler J, et al. 1993. Sonic hedgehog, a member of a family of putative signaling molecules, is implicated in the regulation of CNS polarity. *Cell* 75:1417–30
- Krauss S, Concordet JP, Ingham PW. 1993. A functionally conserved homolog of the *Drosophila* segment polarity gene *hh* is expressed in tissues with polarizing activity in zebrafish embryos. *Cell* 75:1431–44
- Liu C, Peng J, Matzuk MM, Yao HH. Lineage specification of ovarian theca cells requires multicellular interactions via oocyte and granulosa cells. *Nat Commun.* 2015;6:6934.
- Nusslein-Volhard C, Wieschaus E. 1980. Mutations affecting segment number and polarity in *Drosophila*. *Nature* 287:795–801
- Ren Y, Cowan RG, Harman RM, Quirk SM. Dominant activation of the hedgehog signaling pathway in the ovary alters theca development and prevents ovulation. *Mol Endocrinol.* 2009;23(5):711–723.
- Ren Y, Cowan RG, Migone FF, Quirk SM. Overactivation of hedgehog signaling alters development of the ovarian vasculature in mice. *Biol Reprod.* 2012;86(6):174.
- Riddle RD, Johnson RL, Laufer E, Tabin C. 1993. Sonic hedgehog mediates the polarizing activity of the ZPA. *Cell* 75:1401–16
- Russell MC, Cowan RG, Harman RM, Walker AL, Quirk SM. The hedgehog signaling pathway in the mouse ovary. *Biol Reprod.* 2007;77(2):226–236.
- Spicer LJ, Sudo S, Aad PY, Wang LS, Chun S-Y, Ben-Shlomo I, Klein C, Hsueh AJW. The hedgehog-patched signaling pathway and function in the mammalian ovary: a novel role for hedgehog proteins in stimulating proliferation and steroidogenesis of theca cells. *Reproduction.* 2009;138(2):329–339.

Stuart T, Butler A, Hoffman P, Hafemeister C, Papalexi E, Mauck WM 3rd, Hao Y, Stoeckius M, Smibert P, Satija R. Comprehensive Integration of Single-Cell Data. *Cell*. 2019 Jun 13;177(7):1888-1902.e21. doi: 10.1016/j.cell.2019.05.031. Epub 2019 Jun 6. PMID: 31178118; PMCID: PMC6687398.

Wijgerde M, Ooms M, Hoogerbrugge JW, Grootegoed JA. Hedgehog signaling in mouse ovary: Indian hedgehog and desert hedgehog from granulosa cells induce target gene expression in developing theca cells. *Endocrinology*. 2005;146(8):3558–3566.

CHAPTER 3. DECIPHERING CELLULAR INTERACTIONS IN THE OVARY AND POTENTIAL ORIGINS OF THECA CELLS USING SINGLE-CELL TRANSCRIPTOMICS

3.1 Introduction

The ovarian follicle begins as a simple structure made of one germ cell (oocyte) surrounded by a single layer of somatic cell, the pre-granulosa cell. Through specialized and complex communication between the oocyte, granulosa, theca, and stromal cells, ovarian follicles grow, mature, and ovulate. In the bovine, ovulation marks the beginning of the estrous cycle followed by the luteal phase (metestrus and diestrus), that lasts for approximately 17 days. In these 17 days the ovary is under the influence of varying amounts of progesterone. During days 18-21 the ovary is in the follicular phase (proestrus and estrus) and under the growing influence of estrogen. The conversion of androgens to estrogens is imperative for the growth and selection of follicles. As the follicle grows, granulosa cells recruit precursors for theca cells (Edson et al., 2009; Hirshfield et al., 1991). The theca cells are responsible for producing androgens, converted to estrogens by the granulosa cells and providing a feedback loop to regulate steroidogenesis and ultimately the reproductive cycle (Nilsson et al., 2001; Roberts et al., 1990). Although they have an essential role in ovarian function, the exact origin of theca cells is still not completely elucidated. (Erikson et al., 1985; Quattropiani et al., 1973; Young et al., 2010). Theca cells are present in the newborn ovary as thecal stem cells and differentiate from two specific embryonic progenitor cells positive for *Wt1* and *Gli1* that acquire theca lineage markers in response to paracrine signaling (Liu et al., 2015; Honda et al., 2007). Definitive, or terminally differentiated theca cells are not present until after puberty when folliculogenesis begins. Putative thecal stem cells have been isolated from follicles and grown in-vitro and described morphologically to resemble undifferentiated interstitial cells or small fibroblasts (Honda et al., 2007). The signaling required for theca cell recruitment is not completely defined. Utilizing single cell sequencing technology, we identified a definitive theca cell population with an additional population

designated as thecal interstitial cells or putative theca progenitor cells. We investigated ligand-receptor interactions of the theca cells with the other cell clusters within the ovary and identified interactions between the theca interstitial cells and granulosa cells, as well as proliferating cells and definitive theca cells, which could indicate active recruitment of theca cells from the stroma. Finally, we examined how these cell clusters fluctuate over the bovine estrous cycle.

3.2 Materials and Methods

All reagents were purchased from Thermo Fisher Scientific unless otherwise specified.

3.2.1 Animal Preparation

All procedures involving animals were previously approved by the UC Davis Institutional Animal Care and Use Committee. The estrous cycle of four post-pubertal (12-14 months of age), nulliparous heifers of the Angus breed was synchronized prior to slaughter. Estrus synchronization consisted of one injection of 100 µg GnRH (Cystorelin, Merial, Ingelheim am Rhein, Germany) on day 0 together with the placement of an intravaginal device for controlled progesterone release (1.38g, CIDR, Zoetis, Kalamazoo, USA). On day 7, the progesterone-containing device was removed concomitantly with the administration of 25 mg of dinoprost tromethamine (Zoetis, Parsippany-Troy Hills, NJ, USA). Ovaries were examined by ultrasonography starting at day 7 to follow follicle growth and ovulation, and a heat detection patch (product name?) was placed at the base of the tail to aid in estrus detection. Starting at day 7, animals were also observed twice daily for signs of estrus. The day estrus was detected based on behavioral signs of estrus and ultrasonography by the disappearance of the dominant follicle and absence of a corpus luteum was noted as day 1 of the cycle. On day 10 of the cycle, animals had their ovaries examined per rectum and the two heifers with the largest CLs were sacrificed the

following day to harvest ovaries in the mid-luteal phase. The remaining two heifers received a fresh estrus detection patch and were observed for behavioral signs of heat starting at day 16 of the cycle, at which time ultrasonographic scanning of the ovaries was re-started once daily. The diameter of the follicles and corpora lutea were recorded daily to ensure that luteal regression and follicle growth were occurring. At day 20 of the cycle, heifers received 100 µg of GnRH; heifers were sacrificed the following day, corresponding to day 21, to harvest the ovaries during the periovulatory phase of the cycle.

3.2.2 Tissue Processing for single cell-RNA sequencing

Following harvest, the ovaries were immediately taken to the laboratory located across the street from the slaughter plant. Fragments of the outer cortex were dissected 3 mm below the epithelium. Medullar fragments were dissected from the innermost part of the ovary as shown in Fig.6.

3.2.3 Tissue cryopreservation

From both outer cortex and medulla, 300 mg fragments of tissue were placed in a cryovial containing 1 mL of 1.5 M dimethyl sulfoxide (DMSO) and 15% (150µL/mL) fetal bovine serum (FBS) in minimal essential media (MEM) (Gibco Thermo Fisher Scientific). The cryovials were placed in a slow freezer (Cryologic, 1/2-6 Apollo Court Blackburn, Victoria, Australia) to equilibrate at 20 °C for 20 min and then frozen at 0.3 °C/min until -38°C and then moved to LN2 for long term storage. Seeding was done at -7°C. For thawing, the cryovials were placed in a bead bath at 37°C and removed when there was still a large ice chunk in the tube. At this point, the tissue was removed and moved through a 6-well plate containing MEM media at room temperature, 5 min in each well. The tissue

fragments were then minced using scissors into a 50 mL conical tube containing 1 mg/mL of collagenase type IV (Fisher Scientific), 50 mg/mL of Liberase (Thomas Scientific), and 1 U/ml DNase I (Fisher Scientific), in 10 mL of Hanks Balanced Salt Solution with calcium and magnesium (HBSS +/+). This enzyme cocktail was prewarmed to 38°C on the day of tissue dissociation. The tissue was completely minced and then incubated on an orbital shaker at 38 °C for 10 min. Then, the tissue was pipetted up and down (approximately 15x) using a 5 mL serological pipette and put back on the orbital shaker for an additional 10 min. This process was repeated 3 times for complete tissue dissociation. Next, the enzymes were inhibited with 5% FBS, and the cell suspension was filtered through a series of 70 and 30 µm cell strainers. The filter and tube were rinsed using HBSS without calcium and magnesium (HBSS^{-/-}). The suspension was centrifuged at 8°C at 700 x g for 5 minutes at 9 acceleration with no brake. The cells were resuspended in 2 mL of cold HBSS^{-/-} and filtered once more through a 30 µm cell strainer. For cell counting and viability assessment, 50 µl of the suspension were incubated with 50% trypan blue stain for 3 min and examined for viability using a hemocytometer.

3.2.4 Single-Cell RNA Sequencing (scRNAseq) and Data Pre-Processing

The cells were fixed using Parse Biosciences fixation (SB1001) V1.3.0 and single-cell whole-transcriptome (SB2001) kits following the manufacturer's instructions with minor modifications. Once the cells were isolated the centrifugation was increased from 200 x g to 300 x g for 15 min. After fixation and neutralization, the centrifugation was increased to 600 x g. A split pool combinatorial barcoding technique was used for library preparation. The resulting sub-libraries were then sequenced on an Illumina Nextseq6000 for a read depth of an average of 20,000 reads per cell. The Parse Bioscience processing pipeline

(v0.9.6p) was used with default settings to align sequencing reads to the bovine genome ARS-UCD1.2 and to demultiplex samples. Downstream processing was performed using the R package Seurat (v4.3.0) at default settings unless otherwise specified. Cells with fewer than 150 or more than 7,500 detected unique genes, more than 40,000 unique molecular identifiers, or more than 15% mitochondrial reads were excluded from analysis. The resulting gene–cell matrix was normalized and scaled using Seurat’s NormalizeData and ScaleData functions, and principal component analysis was performed with Seurat’s RunPCA function. Utilizing the PCA, an elbow plot is generated using the ElbowPlot function in R, indicating the optimal number of clusters per dataset based on the fit of the data. Cells were clustered using the FindNeighbors (30 dimensions of reduction) and FindClusters (resolution = 0.10 for the medulla and 0.37 for the cortex) functions; for visualizing clusters, RunUMAP (30 dimensions) was run. Wilcoxon rank-sum tests were performed to determine differentially expressed genes between clusters using the FindAllMarkers function (minimal fraction of 25% and log-transformed fold-change threshold of 0.25). The identity of cell clusters was determined by cross-referencing top differentially expressed transcripts with previous studies reporting on single-cell transcriptomes of the ovary as well as referencing the Human Protein Atlas.

3.2.5 Cluster Identification

The FindAllMarkers function was used first to determine the major differentially expressed genes. Following that, the Extract_Top_Markers were utilized to narrow this to the top 5 markers per cluster for further analysis. Using these top 5 markers identified, a clustered dotplot was formed to provide clarity for each cell cluster and their most differentially

expressed genes. Those gene expression profiles are what was used to determine the cell types.

3.2.6 CellChat interactions

CellChat is a database containing interactions among ligands, receptors, and their cofactors that accurately represent known heteromeric molecular complexes. CellChat predicts major signaling inputs and outputs for cells and how those cells and signals coordinate functions using network analysis and pattern recognition. Through manifold learning and quantitative contrasts, CellChat classifies signaling pathways and delineates conserved and context specific pathways across different datasets.

3.3 Results

3.3.1 Cell types of Adult Bovine Ovaries across the Estrous Cycle

Cell clusters were identified by both the top five markers of each cluster as well as characteristic expression of marker genes. Fifteen cell clusters were identified in the cortex: two endothelial clusters (lymph and blood vessels), four immune cell clusters (macrophages, myeloid, T-cells, and B-cells), putative wound regenerative cells, oocytes, theca interstitial cells, theca, smooth muscle, granulosa, stroma, putative migratory stromal cells, and epithelial cells. Seven clusters were identified in the medulla, with four of them identified as subtypes of endothelial cells (angiogenic, forming endothelial tissue, lymphatic and smooth muscle) neuronal, immune and stromal. The UMAPs identifying each cell cluster in the cortex and medulla are shown in Fig. 6.

3.3.2 Changes observed in the cortex and medulla between the follicular and luteal phases of the estrus cycle

When comparing the proportion of cells in the cortex and medulla combined between the peri-ovulatory and mid-luteal phases of the cycle, we did not observe drastic changes in the proportion of cells in the endothelial, immune, epithelial stromal clusters. In contrast, the proliferating cell cluster increased from 0.06% in the peri-ovulatory phase to 0.5% of the total cells in the mid-luteal phase. The theca interstitial cells decreased from 13% in the peri-ovulatory phase to 6% in the luteal phase. Interestingly, the smooth muscle population increased from 9% to 11% between the two phases of the cycle. The granulosa cell population only decreased slightly from the follicular phase 3% to 2% in the luteal phase. We saw a decrease in the number of theca cells from the follicular phase at 1% to the luteal phase at 0.3%. The oocyte population remained almost the same at 0.2% in the follicular phase and 0.1% in the luteal phase. Our putative migratory stromal cell cluster increased from 2% to 3% from the follicular phase to the luteal phase. We see the largest difference in the proliferating cells cluster, in the follicular phase it is a small percentage at 0.06% in the luteal phase it remains a small percentage at 0.5% but the increase is drastic at an 8-fold increase. We observed that in the medulla the proportions of cells did not shift throughout the estrous cycle (Fig.7). In the follicular phase we see endothelial (angiogenic) (42%), endothelial (lymph) (2%), smooth muscle (10%), Forming endothelial (.1%), T-Cells (1%), monocytes (.8%), neuronal (1%), and stromal (ECM)

(40%). In the luteal phase we see endothelial (angiogenic) (42%), endothelial (lymph) (2%), smooth muscle (10%), forming endothelial (.1%), T-Cells (1%), monocytes (.8%), neuronal (1%), and stromal (ECM) (40%).

3.3.3 Cell Cluster Interactions

Using CellChat we identified cell-to-cell interactions between the clusters based on the ligand-receptor interaction database and the cell-cell communication atlas, and we were able to see the endothelial (lymph) cell cluster interacts largely with the putative migratory stromal cells, granulosa, immune (T cells), and putative wound regenerative cells. Interestingly, the putative migratory stromal cells population interacts mostly with the putative wound regenerative cells, and the immune (T cells), and immune (macrophages). Granulosa cells interact mostly with the putative wound regenerative cells, macrophages, Putative Migratory Stromal Cells, and T cells (Fig. 8). Macrophages are mainly interacting with T cells, putative migratory stromal cells, and granulosa cells.

3.4 Discussion

The ovary is a complex organ with multiple functions performed by multiple cell types that have not yet been fully characterized. The experiments described here had two main goals: 1) to identify cells by their unique gene expression profile in the cortex and medulla, examining how cell populations change during the course of the estrus cycle, and 2) to investigate potential origins of ovarian theca cells within the ovarian stroma. Comparing single-cell expression of the cortex and medulla at well-defined stages of the cycle (periovulatory and mid-luteal), our main findings were that the ovarian cortex and medulla

have a different number of cell clusters and we identified unique cell types were identified, including theca interstitial cells, putative migratory stromal cells as well as a population of cells that could be proliferating. We were also able to characterize the 8 cell types in the medulla. As well as identifying the cell types distinguished in the cortex and medulla independently, we were also able to show how these cell proportions change from peri-ovulatory to mid-luteal. The proliferating cell cluster changed the largest with more than an 8-fold increase in percentage of cells within that cluster from the luteal stage to the peri-ovulatory stage. In addition, we were able to identify the presence of the sonic hedgehog pathway within the cortex and evidence for active theca cell recruitment. We were able to utilize a major database of ligands and receptors called CellChat to identify which clusters are communicating with each other. Specifically, we were able to see communication patterns supportive of stromal migration as well as potential theca cell recruitment.

The origins of the theca cells as well as their interactions with the surrounding stroma still remains elusive. Murine theca cells are known to originate from two distinct types of progenitors. One type is represented by Wt1-positive cells found in the fetal ovary, while the other type consists of Gli1-positive cells that migrate from the mesonephros, located adjacent to the ovary (Liu et al., 2015). Close to birth, paracrine signals from granulosa cells, specifically desert hedgehog and Indian hedgehog (IHH), appear to stimulate the expression of Gli1, which serves as a marker for undifferentiated stromal progenitor cells of the theca lineage. The theca cells responsible for androgen production, which are involved in steroidogenesis, may originate from the mesonephros-derived progenitors. On the other hand, theca, fibroblasts, perivascular smooth muscle cells, and potentially

the interstitial ovarian cells may arise from the ovarian WT1+ progenitors (Richards et al., 2018). In our dataset, we see expression of *IHH* within the granulosa cell population, *PTCH1*, *SMO*, *GLI1*, *HHIP*, and *TCF21* all expressed within the theca cell cluster (Fig.9). James et al (2023) describes three discrete subtypes of theca cells that arise from the stroma, a structural theca cell, a perifollicular theca cell and androgenic theca cell. They describe a model of theca differentiation, the cells further from the follicle (structural theca cells) express TCF21, the closer the cells get to the follicle the more NR5A1 that is expressed (James et al., 2023). We see high expression of TCF21 in the theca stromal population, albeit a small number expressing it and a lesser amount expressed in the theca population while NR5A1 is expressed highly in the theca population. Our data seems to support what they show, although more follow up is needed. In the current study using young adult bovine ovaries, we identified 16 separate clusters in the ovarian cortex as well as 8 cell clusters in the medulla and how their proportions change during the follicular phase and luteal phase of the estrous cycle. We see the largest change in the proliferating cell cluster from the follicular phase to the luteal phase. After ovulation, newly formed blood vessels proliferate through the basement membrane between the theca and granulosa cells. This rapid proliferation is to support the growing corpus luteum and sustain its function (Tamanini et al., 2004) and our data strongly supports this long-known concept. Angiogenesis typically consists of three stages, breakdown of the basement membrane, migration of endothelial cells, proliferation of endothelial cells to establish a new blood vessel sprout (Redmer et al., 2001). This large growth event is likely the reason we see this almost 200% increase in cells. The number of cells is still low, only .5% of the cortex. In the primate, most of the dividing cells (~85% in the early

luteal phase) are endothelial cells (Stouffer et al., 2001). The duration of intense proliferation of endothelial cells varies across species (Stouffer et al., 2001)

While single-cell sequencing studies offer detailed insights into the nuances of various ovarian cellular populations, including the stroma, it is important to continually consider the potential limitations of the chosen starting cellular populations, such as focusing solely on the outer cortex. Identification of cell populations in the medulla of the ovary has yet to be done in any other species. In this study, we define a large cluster of endothelial cells responsible for blood vessels, smooth muscle, forming blood vessels, and lymphatic vessels; two immune cell clusters, a neuronal cell cluster and finally a stromal population. As the medulla houses the majority of vasculature in the ovary it is unsurprising that this is a large portion of the medullary cells. The stromal cluster is the other majority of the medullary cells and is defined by the ECM remodeling genes they express, Spondin 1 (SPON1) and Glypican 6 (GPC6). SPON1 is predicted to be involved in cell adhesion and co-localizes with collagen-containing extracellular matrix where GPC6 has been implicated in the control of cell growth and cell division (Cudmore et al., 2011; Filmus et al., 2020). Co-expression of these genes with various collagens could potentially mean these cells could be integral for ECM deposition.

Overall, our study contributes to our understanding of the ovarian cellular landscape, shedding light on the intricacies of cell types, their origins, and their dynamic changes during the estrus cycle. This is particularly true for the ovarian medulla, which we have described for the first time, and which had not been extensively characterized in previous research. Further research is needed to explore the functional implications of these findings in reproductive biology.

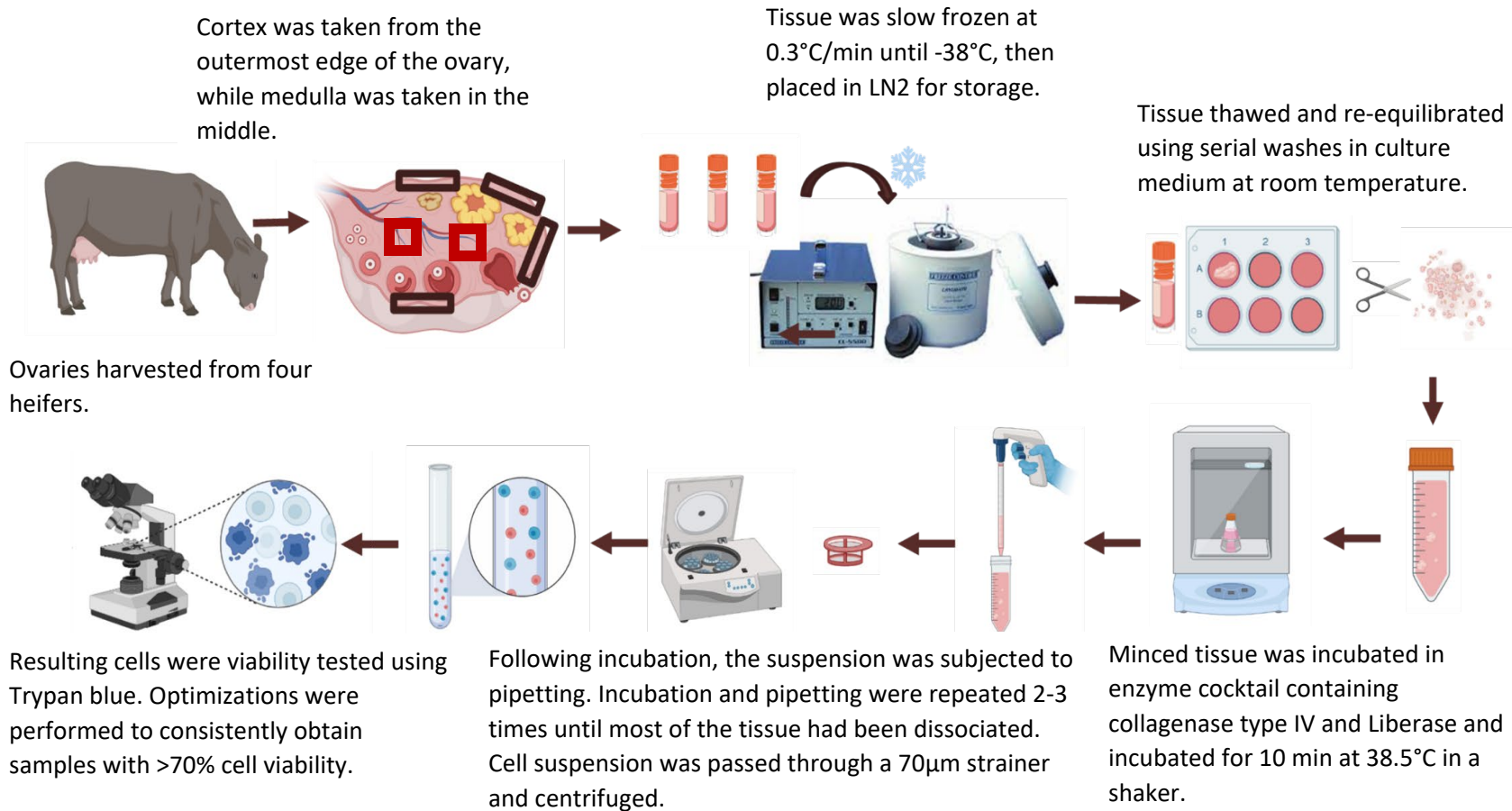
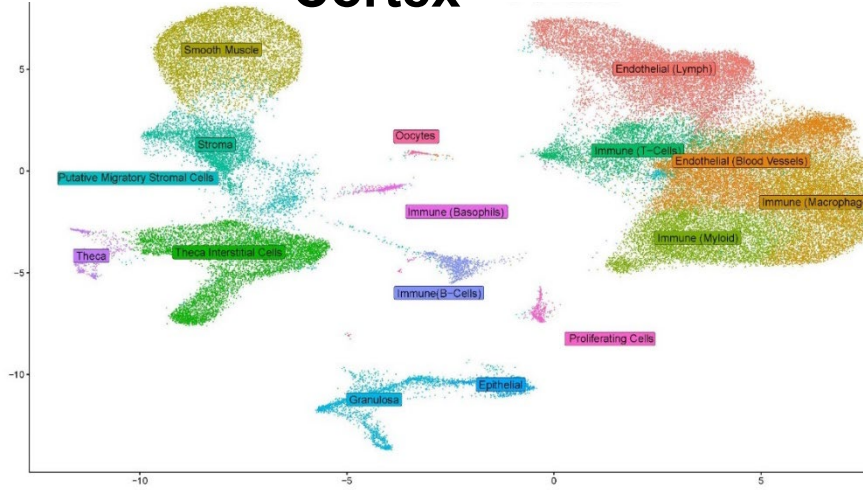
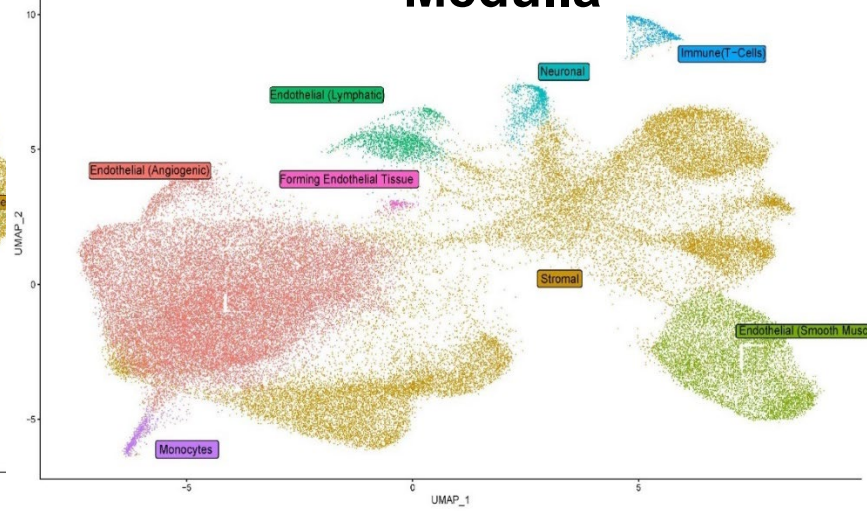


Figure 6: Single cell isolation protocol. Ovaries were harvested from four heifer at either the luteal phase of the estrous cycle or the follicular phase of the estrous cycle. After dissection the cortex and medulla were slow frozen and stored in LN2. The tissue fragments were thawed and re-equilibrated using serial washes to bring the tissue temperature up slowly. The tissue was minced and incubated in an enzyme cocktail of collagenase type IV and Liberase for ten minutes at 38.5°C in an orbital shaker. Following incubation, the suspension was subjected to pipetting with a serological pipette to break the tissue apart. Once the tissue has been dissociated, the cell suspension was passed through a 70µm cell strainer then a 30µm strainer and then centrifuged. The resulting cell suspension were then viability tested.

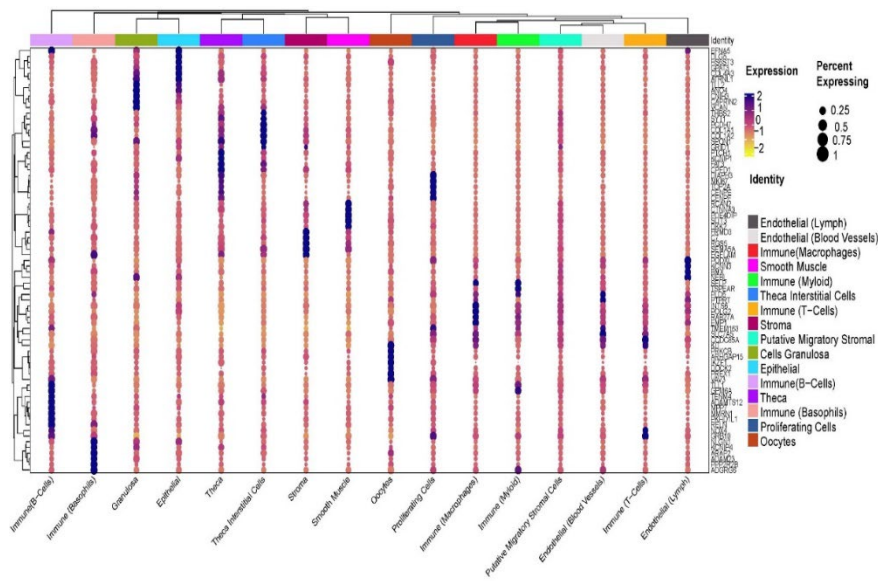
A.1. **Cortex**



B.1. **Medulla**



A.2



B.2

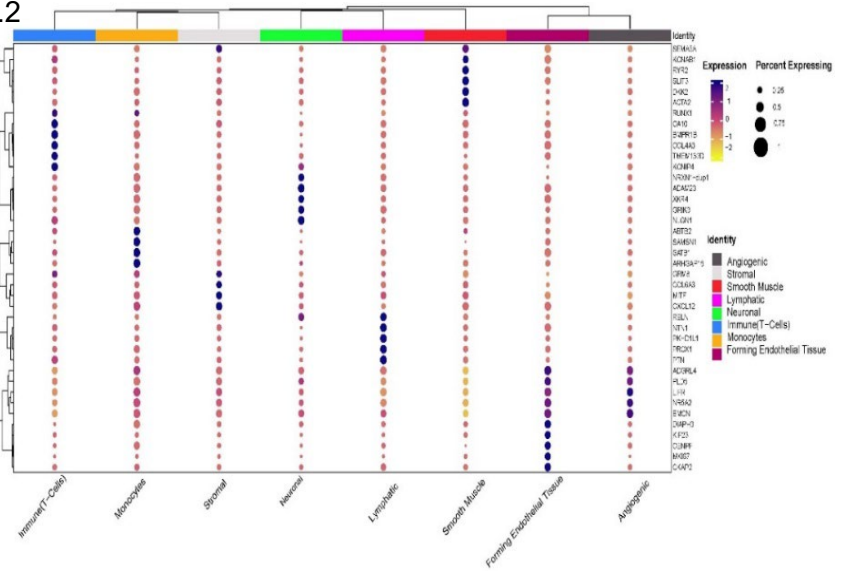
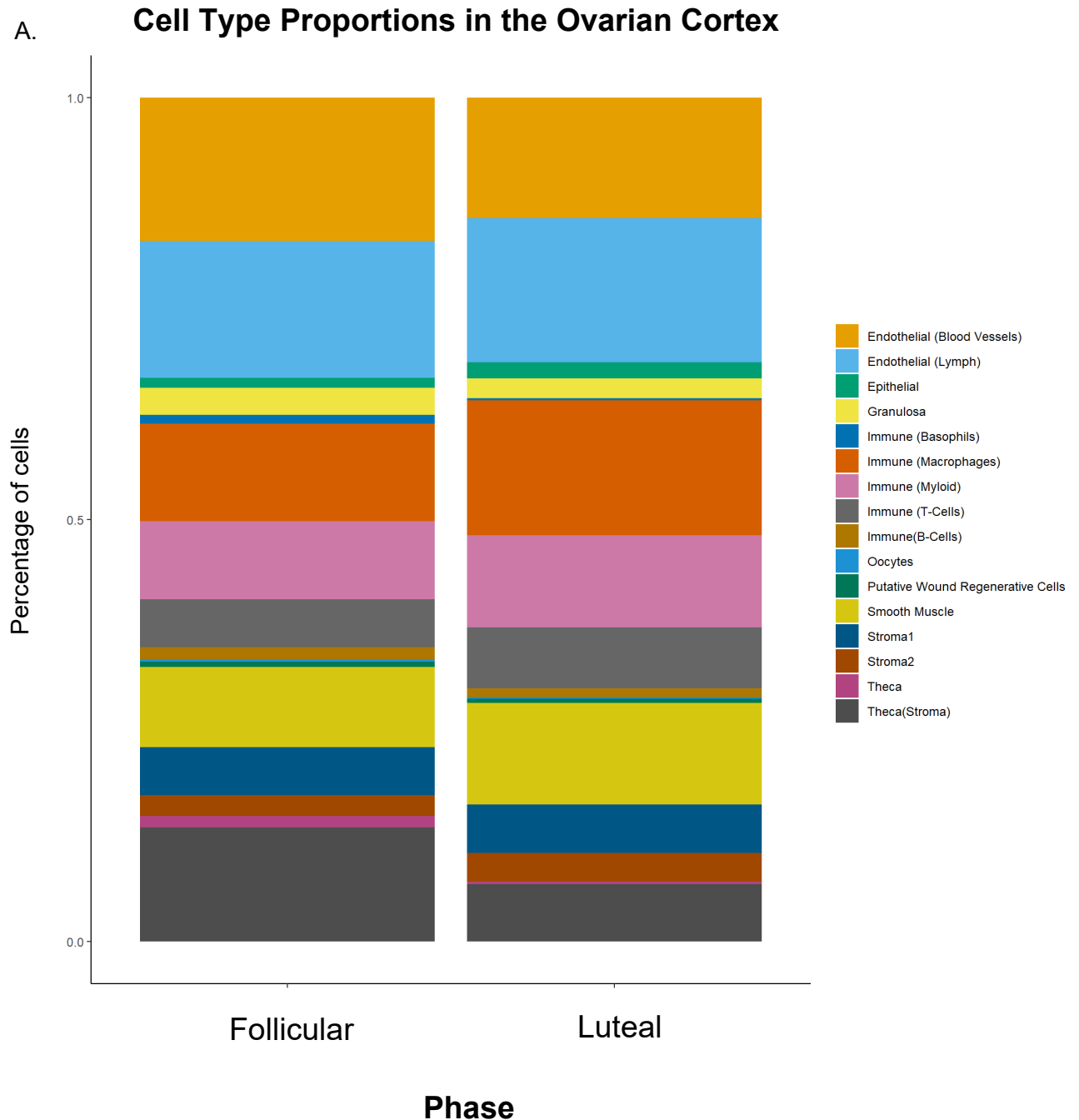


Figure 7: Cell distribution in the Bovine Ovarian Cortex: A) 1 The sixteen cell cluster types within the bovine ovarian cortex shown in a uniform manifold approximation and projection. **A) 2** The top 5 expressed genes in the bovine ovarian cortex determined by a Wilcoxon Rank Sum test and showcased as a clustered dotplot. The percentage of cells expressing the gene are noted by dot size and expression level noted by color. **B) 1** The eight cell clusters in the bovine ovarian medulla shown in a uniform manifold approximation and projection. **B) 2** The top 5 expressed genes in the bovine ovarian medulla determined by a Wilcoxon Rank Sum test and shown as a clustered dotplot.



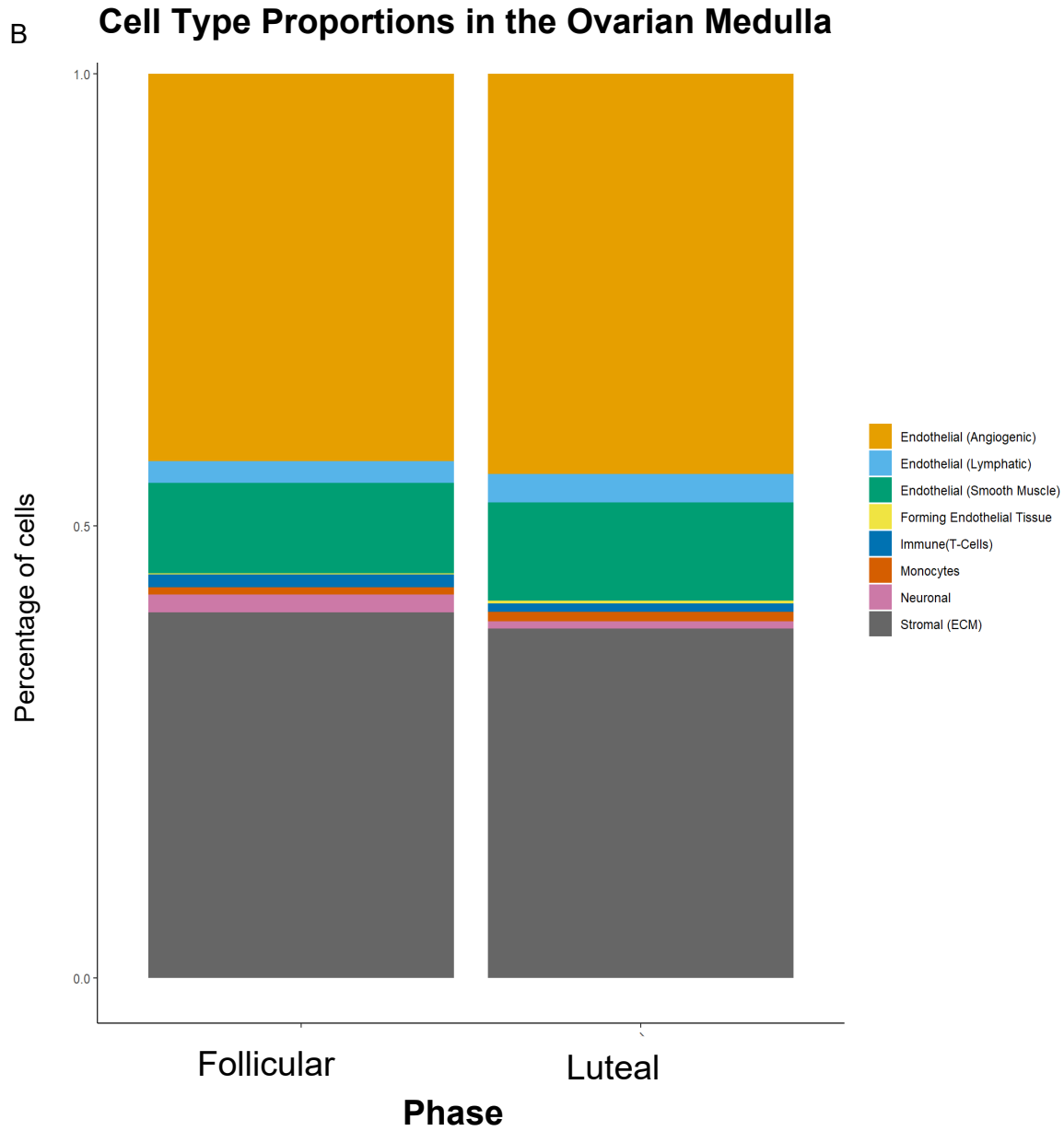
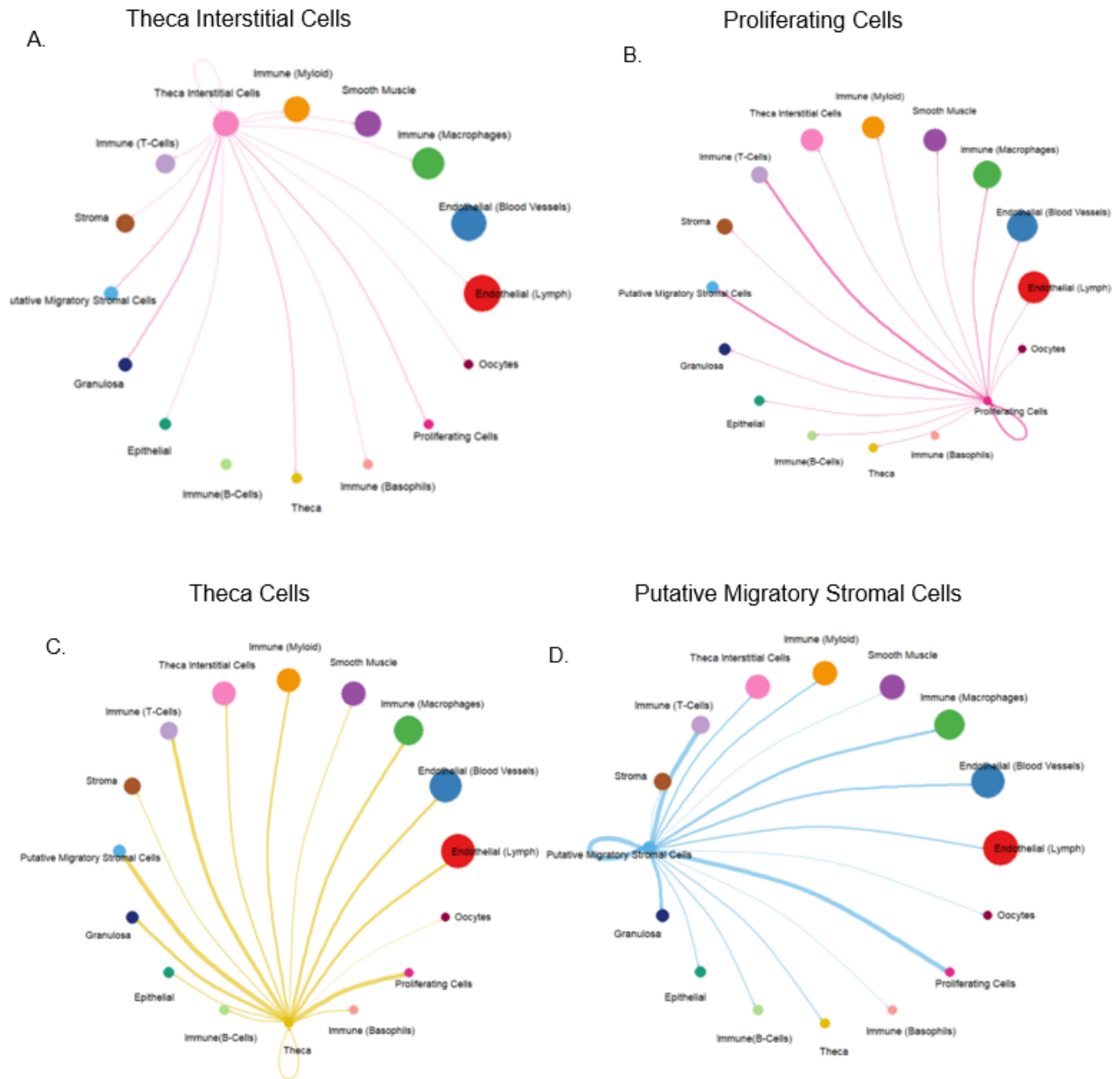


Figure 8: Cell Type Proportions in the Follicular vs Luteal Phase: A) The cortex cell types and proportions in both the follicular and luteal phase of the estrous cycle. **B)** The medulla cell types in both the follicular and luteal phase of the estrous cycle.

CellChat Interactions



Granulosa Cells

E.

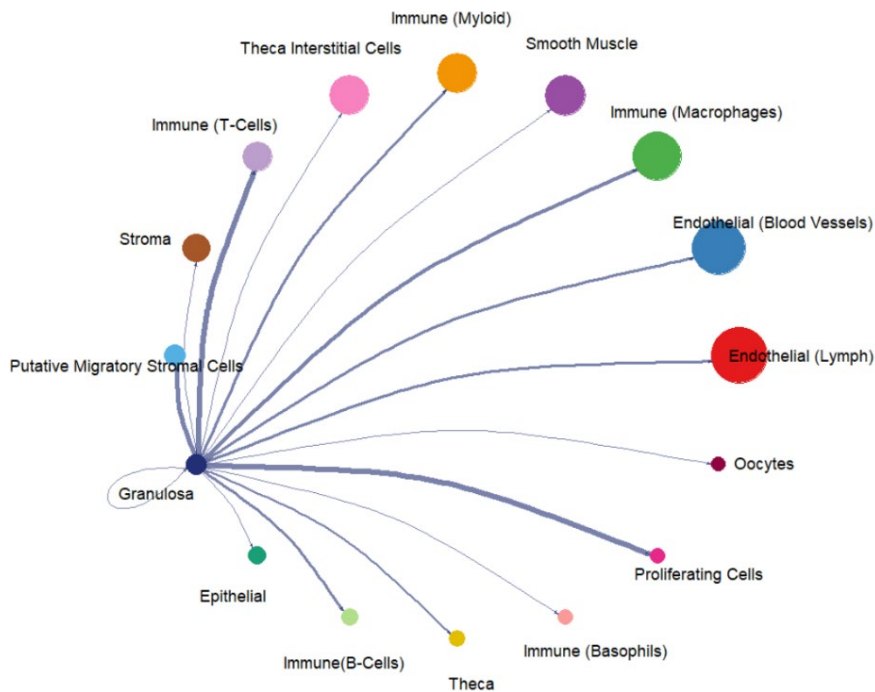


Figure 9: CellChat interactions. The cell-cell communication network for five of the cell clusters in the cortex utilizing a database of ligand-receptor interactions. **A.** The theca interstitial cells are communicating the strongest with the granulosa cells, the proliferating cells, the putative migratory stromal cells, theca cells as well as immune cells. **B.** The proliferating cells are communicating the strongest with the putative migratory stromal cells as well as immune cells. **C.** Theca cells are communicating with several other clusters, the strongest with; granulosa cells, immune cells (T-cells), putative migratory stromal cells, and proliferating cells. Additionally, they are communicating at a smaller amount with; endothelial cells (lymph, and blood vessels) and macrophages. **D.** Putative migratory stromal cells are strongly communicating with proliferating cells and granulosa cells. **E.** Finally, the granulosa cells are interacting the strongest with immune cells (macrophages), putative migratory stromal cells, and proliferating cells. They are also communicating to a lesser extent with theca cells and endothelial cells.

Sonic Hedgehog Signaling in the Bovine Ovarian Cortex

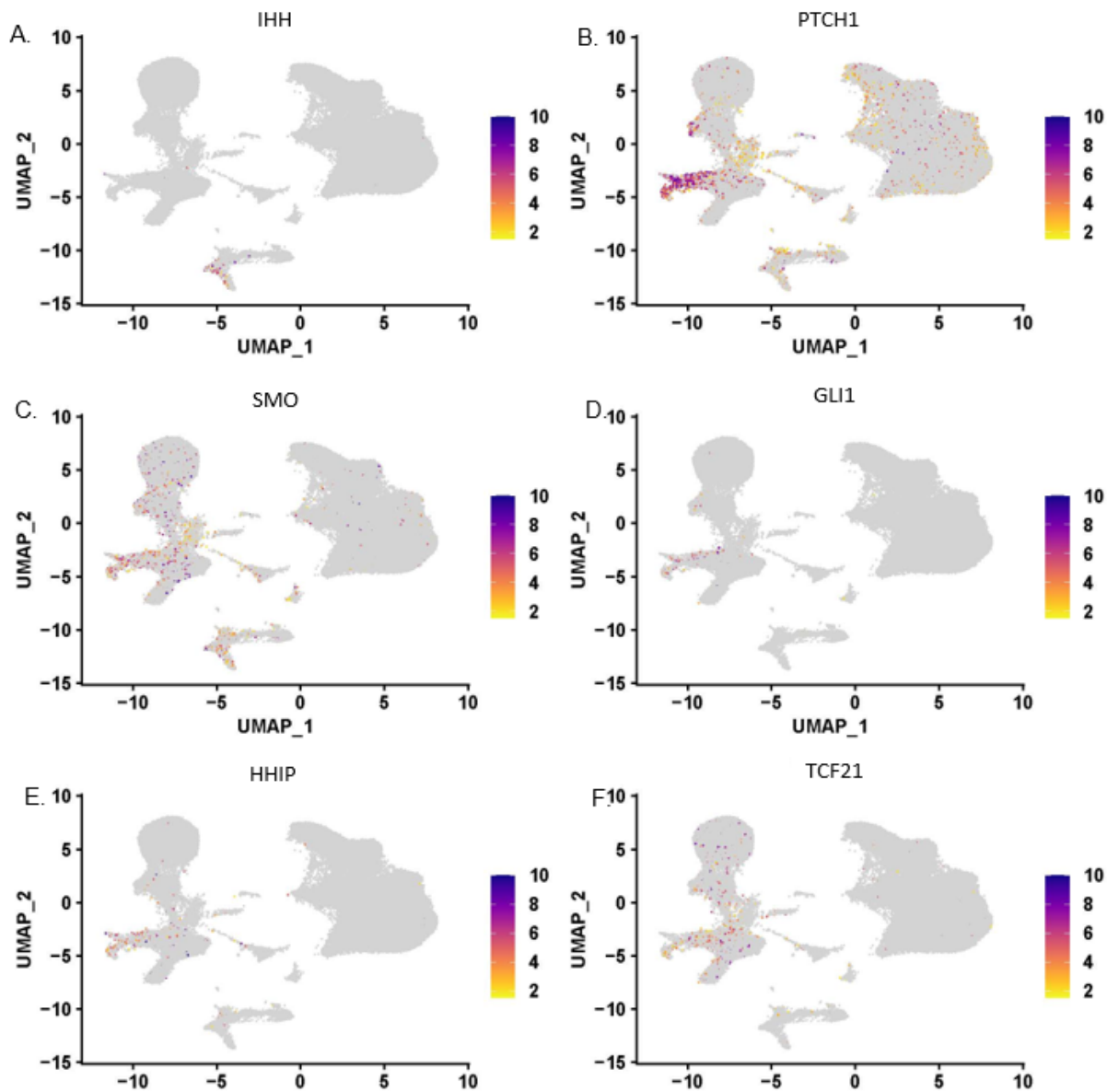


Figure 10: Sonic Hedgehog Signaling in the Bovine Ovarian Cortex. A. Expression localization of IHH. B. Expression localization of PTCH1. C. Expression localization of SMO. D. Expression localization of GLI1. E. Expression localization of HHIP. F. Expression localization of TCF21.

CHAPTER 4. CONCLUSION TO THE DISSERTATION

This dissertation provides valuable insights into the complex nature of the ovary and its diverse cell populations. Using single-cell RNA sequencing, our studies aimed to understand how these cells change during the estrus cycle and investigate the origins of theca cells.

Key findings include the identification of unique cell types, such as thecal? interstitial cells and migratory stromal cells, and observations of significant changes in cell proportions from the follicular to luteal phases. The presence of the hedgehog signaling pathway in the cortex supports its role in theca cell recruitment.

Furthermore, these studies explored medullary cell populations, revealing the presence of endothelial cells, smooth muscle cells, immune cells, neuronal cells, and stromal cells, particularly those involved in extracellular matrix remodeling. The luteal phase showed intense proliferation of endothelial cells, crucial for angiogenesis and corpus luteum function.

While this research sheds light on ovarian complexity, it also acknowledges the importance of considering potential limitations in transcriptomic data. Future studies will delve deeper into the functional implications of these findings for reproductive biology and assisted reproductive technologies.

REFERENCES

4.1 References

Abd-Elkareem M 2017 Cell-specific immuno-localization of progesterone receptor alpha in the rabbit ovary during pregnancy and after parturition. *Animal Reproduction Science* 180 100–120. (<https://doi.org/10.1016/j.anireprosci.2017.03.007>)

Candelaria NR, Padmanabhan A, Stossi F, Ljungberg MC, Shelly KE, Pew BK, Solis M, Rossano AM, McAllister JM & Wu S et al. 2019 VCAM1 is induced in ovarian theca and stromal cells in a mouse model of androgen excess. *Endocrinology* 160 1377–1393. (<https://doi.org/10.1210/en.2018-00731>)

Edson, M. A., Nagaraja, A. K. & Matzuk, M. M. The mammalian ovary from genesis to revelation. *Endocr. Rev.* 30, 624–712 (2009).

Friedman HS, Dolan ME, Kaufmann SH, et al. Elevated DNA polymerase alpha, DNA polymerase beta, and DNA topoisomerase II in a melphalan-resistant rhabdomyosarcoma xenograft that is cross-resistant to nitrosoureas and topotecan. *Cancer Res.* 1994;54(13):3487–3493.

Hirshfield, A. N. Development of follicles in the mammalian ovary. *Int. Rev. Cytol.* 124, 43–101 (1991).

Hummitzsch K, Hatzirodos N, Macpherson AM, Schwartz J, Rodgers RJ and Irving-Rodgers HF 2019. Transcriptome analyses of ovarian stroma: tunica albuginea, interstitium and theca interna. *Reproduction* 157 545–565.

Kenngott RAM, Scholz W & Sinowatz F 2016 Ultrastructural aspects of the prenatal bovine ovary differentiation with a special focus on the interstitial cells. *Anatomia, Histologia, Embryologia* 45 357–366. (<https://doi.org/10.1111/ahe.12203>)

Irving-Rodgers HF & Rodgers RJ 2006 Extracellular matrix of the developing ovarian follicle. *Seminars in Reproductive Medicine* 24 195–203. (<https://doi.org/10.1055/s-2006-948549>)

Jabara S, Christenson LK, Wang CY, McAllister JM, Javitt NB, Dunaif A & Strauss JF 2003 Stromal cells of the human postmenopausal ovary display a distinctive biochemical and molecular phenotype. *Journal of Clinical Endocrinology and Metabolism* 88 484–492. (<https://doi.org/10.1210/jc.2002-021274>)

Konishi I, Fujii S, Okamura H, Parmley T & Mori T 1986 Development of interstitial cells and ovigerous cords in the human fetal ovary: an ultrastructural study. *Journal of Anatomy* 148 121–135.

Liu C, Peng J, Matzuk MM & Yao HHC 2015 Lineage specification of ovarian theca cells requires multicellular interactions via oocyte and granulosa cells. *Nature Communications* 6 6934. (<https://doi.org/10.1038/ncomms7934>)

Magoffin, D. A. The ovarian androgen-producing cells: a 2001 perspective. *Rev. Endocr. Metab. Disord.* 3, 47–53 (2002).

Nilsson, E. & Skinner, M. K. Cellular Interactions That Control Primordial Follicle Development and Folliculogenesis. *J. Soc. Gynecol. Investig.* 8, S17–S20 (2001).

Richards JS, Ren YA, Candelaria N, Adams JE & Rajkovic A 2018 Ovarian follicular theca cell recruitment, differentiation, and impact on fertility: 2017 update. *Endocrine Reviews* 39 1–20. (<https://doi.org/10.1210/er.2017-00164>)

Tingen CM, Kiesewetter SE, Jozefik J, Thomas C, Tagler D, Shea L and Woodruff TK 2011. A macrophage and theca cell-enriched stromal cell population influences growth and survival of immature murine follicles in vitro. *Reproduction* 141 809–820.

Stastna J, Pan X, Wang H, et al. Differing and isoform-specific roles for the formin DIAPH3 in plasma membrane blebbing and filopodia formation. *Cell Res.* 2012;22(4):728–745. doi:10.1038/cr.2011.202

Shiina, H. et al. Premature ovarian failure in androgen receptor-deficient mice. *Proc. Natl Acad. Sci. USA* 103, 224–229 (2006).

Wagner M, Yoshihara M, Douagi I, Damdimopoulos A, Panula S, Petropoulos S, Lu H, Petterson K, Palm K & Katayama S et al. 2020 Single-cell analysis of human ovarian

cortex identifies distinct cell populations but no oogonial stem cells. *Nature Communications* 11 1147. (<https://doi.org/10.1038/s41467-020-14936-3>)

Wang S, Zheng Y, Li J, Yu Y, Zhang W, Song M, Liu Z, Min Z, Hu H & Jing Y et al. 2020 Single-cell transcriptomic atlas of primate ovarian. *Aging Cell* 180 585-600.e19. (<https://doi.org/10.1016/j.cell.2020.01.009>)

Wang, P. H. & Chang, C. Androgens and ovarian cancers. *Eur. J. Gynaecol. Oncol.* 25, 157–163 (2004).

Young, J. M. & McNeilly, A. S. Theca: the forgotten cell of the ovarian follicle. *Reproduction* 140, 489–504 (2010).